Mathematical Biosciences and Engineering

http://www.aimspress.com/journal/mbe

MBE, 20(8): 15094–15119.
DOI: 10.3934/mbe.2023676
Received: 21 April 2023
Revised: 28 May 2023
Accepted: 04 July 2023
Published: 17 July 2023

Research article

Exploration on dynamics in a ratio-dependent predator-prey bioeconomic model with time delay and additional food supply

Ting Yu, Qinglong Wang*and Shuqi Zhai

School of Mathematics and Statistics, Hubei Minzu University, Enshi 445000, China

* **Correspondence:** Email: qlwang@hbmzu.edu.cn; Tel: +8618986850008.

Abstract: In this manuscript, a novel ratio-dependent predator-prey bioeconomic model with time delay and additional food supply is investigated. We first change the bioeconomic model into a normal version by virtue of the differential-algebraic system theory. The local steady-state of equilibria and Hopf bifurcation could be derived by varying time delay. Later, the formulas of the direction of Hopf bifurcation and the properties of the bifurcating periodic solutions are obtained by the normal form theory and the center manifold theorem. Moreover, employing the Pontryagin's maximum principle and considering the instantaneous annual discount rate, the optimal harvesting problem of the model without time delay is analyzed. Finally, four numeric examples are carried out to verify the rationality of our analytical findings. Our analytical results show that Hopf bifurcation occurs in this model when the value of bifurcation parameter, the time delay of the maturation time of prey, crosses a critical value.

Keywords: predator-prey bioeconomic model; ratio-dependent; time delay; Hopf bifurcation; optimal harvesting

1. Introduction

There are some relationships between species such as predation, competition, mutualism and parasitism, while predation is a popular representative in ecosystem. Since Lotka [1] and Volterra [2] almost simultaneously proposed the Lotka-Volterra model of predation between two populations, many scholars have studied the dynamics of different types of predator-prey models (see [3–6]). They usually consider the response of the predator to the prey density changing through a functional response in the modelling of predator-prey model. A variety of models are generated due to the selection of different types of functional response functions. Holling type I, II and III [7–9] were first proposed by Holling based on empirical field data from 1959 to 1966. The traditional predator-prey models assumed that the functional response depends only on the prey populations [10–12]. However, several biologists questioned functional response is determined solely by prey density. They suggested that predators might interfere with each other's foraging because predators share or compete for food with each other when predatos forage. Therefore, the functional response should depend not only on the prey density but also on the predator, see for instance [13–22]. The authors considered that the growth of population is on slow time scale (days or months) and established the ratio-dependent model. By virtue of Holling type II function, Kesh et al. [19] proposed a ratio-dependent model and obtained the sufficient condition for permanent co-existence. Xu and Chen [20] and Tang and Chen [21] studied the local and global stability of two classes of ratio-dependent system with delay, respectively. Fan and Li [22] proposed a delayed discrete ratio-dependent model and obtained the sufficient conditions for the permanence.

The study on providing additional food for the predator is an important topic in ecological modeling, which leads to more complex dynamics for the predator-prey model and has received extensive attentions. In recent years, many scholars have focused on the work of providing additional food for the predator to protect species or control pest, for details to see references [23–26]. Assuming that the quality of the additional food remains constant, Srinivasu and Prasad [23] found that the growth of the predator could be enhanced by the provision of extra food for the predator. Basheer et al. [24] showed that providing extra food for the predator is effective in eliminating pests. Samaddar [25] and Wu [26] investigated the Hopf bifurcation of the model which took into account the provision of extra food for the predator and time delay.

Motivated by the view of Arditi and Ginzburg [27] and Srinivasu et al. [28], a ratio-dependent model which involves the assumption that the additional food is provided for the predator was first proposed by Kumar and Chakrabarty [29]. This extra food is considered to be available uniformly within the ecological domain [28]. The model is as follows

$$\begin{cases} \dfrac{dN}{dT} = rN\Big(1 - \dfrac{N}{K}\Big) - \dfrac{e_1(\frac{N}{P})}{1 + e_1h_1(\frac{N}{P}) + e_2h_2(\frac{A}{P})}P, \\ \dfrac{dP}{dT} = \dfrac{n_1e_1(\frac{N}{P}) + n_2e_2(\frac{A}{P})}{1 + e_1h_1(\frac{N}{P}) + e_2h_2(\frac{A}{P})}P - m'P. \end{cases} \tag{1.1}$$

Where A is the additional food for the predator, the number of preys and predators at time T is respectively represented by $N(T)$ and $P(T)$, here $N(0) > 0, P(0) > 0$. The intrinsic growth rate of the prey is expressed by r and m' stands for natural mortality of the predator, the carrying capacity of the prey is described by K. e_1 and e_2 denote the coefficients of predator capture on prey and additional food, n_1 and n_2 represent separately the nutritional value of the prey and additional food, h_1 and h_2 are handling time per predator per unit of the ratio $\frac{N}{P}$ prey biomass and per predator per unit of the ratio $\frac{A}{P}$ additional food biomass, respectively.

Another important aspect, the real ecosystem could not be denied the fact that the processes of biological development are not normally instantaneous on account of the interaction with environment or other species. Therefore, several biologists and mathematicians began to explore and study the time-delay models inspired by the dynamics of population models with time delay. From the biological and mathematical point of view, predator-prey models with delay [30–35] tend to exhibit more complex dynamics than those without that, such as local and global stability, Hopf bifurcation, limit cycle and so on. For example, the properties of the periodic solutions of the model with delay and impulse were obtained in [31]. Jiang [34] investigated the global asymptotical and the existence of Hopf bifurcation of a diffusive model with ratio-dependent function and delay. By studying the delay differential system, Tang and Zhang [35] showed that the stability of the model becomes unstable state when the time reaches a certain critical point, thus Hopf bifurcation occurs. Considering the maturation time of the prey, model (1.1) turns to the following version

$$\begin{cases} \dfrac{dN}{dT} = rN\Big(1 - \dfrac{N(T-\tau)}{K}\Big) - \dfrac{e_1(\frac{N}{P})}{1 + e_1h_1(\frac{N}{P}) + e_2h_2(\frac{A}{P})}P, \\ \dfrac{dP}{dT} = \dfrac{n_1e_1(\frac{N}{P}) + n_2e_2(\frac{A}{P})}{1 + e_1h_1(\frac{N}{P}) + e_2h_2(\frac{A}{P})}P - m'P. \end{cases} \tag{1.2}$$

It is widely known that human survival and development depend on natural resources. Biological resources have the most unique development mechanism due to renewability. Over-exploitation of biological resources will not only lead to a reduction in their quantity and quality, but also may drive species to extinction. Thus, taking the path of sustainable development becomes necessary to maintain ecological balance and meets the material needs of the people. From an economic perspective, the impact of harvesting effort on ecosystem guarantees that the net economic revenue is equal to the difference between total revenue and total cost which may influence on the harvesting activities. There has been a growing literature for the modeling and analysis of bioeconomic systems. The existence of steady state was discussed in a bioeconomic model with ratio-dependent [36]. The dynamics of the delay and diffusion terms of a bioeconomic plankton model was investigated by Zhao et al. [37]. In particular, an increasing number of bioeconomic models are expressed by differential-algebraic equations [38–44]. A prey-predator economic model with time-delay and stage structure was proposed by Zhang et al. [38]. Through detailed proof, the results show that the model undergoes three different bifurcational phenomena. Chen [41] established a biological economic model which suggested that the model undergoes flip bifurcation and Neimark-Sacker bifurcation.

To extend the model above, a bioeconomic model with time delay incorporating two differential equations and one algebraic equation is written as

$$\begin{cases} \dfrac{dN}{dT} = rN\Big(1 - \dfrac{N(t-\tau)}{K}\Big) - \dfrac{e_1(\frac{N}{P})}{1 + e_1h_1(\frac{N}{P}) + e_2h_2(\frac{A}{P})}P, \\ \dfrac{dP}{dT} = \dfrac{n_1e_1(\frac{N}{P}) + n_2e_2(\frac{A}{P})}{1 + e_1h_1(\frac{N}{P}) + e_2h_2(\frac{A}{P})}P - m'P - q_1EP, \\ E(p_1q_1P - w) - Q = 0. \end{cases} \tag{1.3}$$

From an economic perspective, the impact of harvesting effort on ecosystem is expressed as: net economic revenue (NER) = total revenue (TR) - total cost (TC). TR = $p_1q_1E(t)P(t)$ and TC = $wE(t)$, where p_1 is the price per unit predator biomass, q_1 and $E(t)$ stand for the harvesting capacity coefficient and harvesting effort of the predator, respectively. w represents the cost per unit predator harvesting efforts. Q means the NER. We only consider the harvesting of the predator, the catch rate function $h(t)$ is written as $h(t) = q_1E(t)P(t)$ which meets the catch-per-unit-effort hypothesis [45]. All the parameters in model (1.3) are positive. The initial conditions for model (1.3) are given $N_{[-\tau,0]} \in C_+([-\tau, 0], \mathbb{R}_+)$. If $P(0)$ is provided, $E(0)$ can be expressed as $Q/(p_1q_1P(0) - w)$ thus it is content with $P(0) > w/p_1q_1$.

Significantly, a real-life application is motivated by data from Katz [46]. We consider that prey N is represented by barnacles Balanus balanoides and predator P is expressed as snails Urosalpinx cinerea. The data strongly supports the ratio-dependent form N/P much better than that only depends on prey N. Incorporating additional food A (Ostrea gigas thunberg) into our model, our target is to address our understanding on the consequences of providing additional food for the predator on the dynamics, which brings out an explicit link between practical biological control and theoretical fruits. Besides, we investigate the optimal harvesting strategy of snails Urosalpinx cinerea due to its use as a kind of Chinese medical herbs.

The rest of this manuscript is emerged as follows. Section 2 is devoted to discussing the local steady-state and the Hopf bifurcation by investigating the characteristic equation. In Section 3, the main results including the properties of the bifurcating periodic solutions and the formulas of the direction of Hopf bifurcation are investigated. The optimal harvesting problem of model (1.3) without time delay is analyzed in Section 4. Four numerical examples are displayed in Section 5 to explain our findings. The brief and powerful biological discussion and conclusions are provided in Section 6. The paper end with Appendices A, B and C to show some proof and calculations.

2. Local stability of equilibria and Hopf bifurcation

Model (1.3) is simplified and analyzed by using the following rescaling

$$x = \frac{N}{K}, y = \frac{P}{Ke_1h_1}, t = rT.$$

After nondimensionalizing the model (1.3) for convenience, we obtain

$$\begin{cases} \dfrac{dx}{dt} = x(1 - x(t-\tau)) - \dfrac{cxy}{x + y + \alpha\xi}, \\ \dfrac{dy}{dt} = \dfrac{b(x+\xi)y}{x + y + \alpha\xi} - my - qEy, \\ E(pqy - w) - Q = 0, \end{cases} \tag{2.1}$$

where $c = \frac{e_1}{r}$, $\alpha = \frac{n_1h_2}{n_2h_1}$, $\xi = \frac{\gamma A}{K}$, $\gamma = \frac{n_2e_2}{n_1e_1}$, $b = \frac{n_1}{rh_1}$, $m = \frac{m'}{r}$, $q = \frac{q_1}{r}$, $p = p_1Ke_1h_1r$.

Through calculation, the internal equilibrium of the model (2.1) could be written as $P_0^*(x^*, y^*, E^*)$, where

$$E^* = \frac{Q}{pqy^* - w}, \quad y^* = \frac{x^{*2} - x^* + \alpha\xi x^* - \alpha\xi}{1 - x^* - c}$$

and x^* is the positive solution of $Ax^4 + Bx^3 + Cx^2 + Dx + F = 0$ where

$$\begin{aligned} A =&pqb, \qquad B = -2pqb + pqb\alpha\xi + wb + pqbc + pqb\xi - pqmc, \\ C =&pqb - 2pqb\alpha\xi - 2wb + 2wbc - pqbc + pq\alpha\xi bc - 2pqb\xi + pqb\alpha\xi^2 + wb\xi + pqbc\xi + pqmc \\ &- 2pq\alpha\xi mc - wmc + qQc, \\ D =&pqb\alpha\xi + wb - 2wbc - pqbc\alpha\xi + wbc^2 + pqb\xi - pqb\alpha\xi^2 - 2wb\xi - pqb\alpha\xi^2 + 2wbc\xi - pqbc\xi \\ &+ pqbc\alpha\xi^2 + 2pq\alpha\xi mc + wmc - wc^2m - pq\alpha^2\xi^2mc - wmc\alpha\xi - qQc + qQc\alpha\xi + qQc^2, \\ F =&pq\alpha\xi^2b + wb\xi - 2wcb\xi - pqbc\alpha\xi^2 + wc^2b\xi + pq\alpha^2\xi^2mc + wmc\alpha\xi - wmc^2\alpha\xi - qQc\alpha\xi \\ &+ qQc^2\alpha\xi. \end{aligned}$$

Remark 2.1. By Descartes sign rule [47], the possible positive roots of equation $Ax^4 + Bx^3 + Cx^2 + Dx + F = 0$ are as follows.

(i) If any one of the conditions (a), (b), (c) and (d) holds, the equation exists one positive root

$$\begin{aligned}&(a)\;\; A<0,B>0,C>0,D>0,F>0; \;\; (b)\;\; A>0,B>0,C>0,D>0,F<0;\\&(c)\;\; A<0,B<0,C>0,D>0,F>0; \;\; (d)\;\; A>0,B>0,C>0,D<0,F<0.\end{aligned}$$

(ii) If any one of the conditions (e), (f), (g), (h), (i) and (j) holds, the equation exists two positive roots or no roots

$$\begin{aligned}&(e)\;\; A>0,B<0,C>0,D>0,F>0; \;\; (f)\;\; A>0,B>0,C<0,D>0,F>0;\\&(g)\;\; A>0,B>0,C>0,D<0,F>0; \;\; (h)\;\; A<0,B>0,C>0,D>0,F<0;\\&(i)\;\; A>0,B<0,C<0,D>0,F>0; \;\; (j)\;\; A>0,B>0,C<0,D<0,F>0.\end{aligned}$$

(iii) If any one of the conditions (k), (l), (m) and (n) holds, the equation exists three positive roots or one positive root

$$\begin{aligned}&(k)\;\; A<0,B>0,C<0,D>0,F>0; \;\; (l)\;\; A<0,B>0,C>0,D<0,F>0;\\&(m)\; A>0,B<0,C>0,D>0,F<0; \;\; (n)\;\; A>0,B>0,C<0,D>0,F<0.\end{aligned}$$

(iv) If the condition (p) holds, the equation exists four positive roots or two positive roots or no roots

$$(p)\;\; A>0,B<0,C>0,D<0,F>0.$$

According to the following theorem, we know the conditions of the Hopf bifurcation occurs in model (2.1).

Theorem 2.1. If the assumptions $A_1+A_4>0, A_3>0, A_2+A_3>0$ and $A_2-A_3<0$ are satisfied, then when $\tau<\tau_0$, equilibrium $P_0^*(x^*,y^*,E^*)$ of model (2.1) is stable; equilibrium $P_0^*(x^*,y^*,E^*)$ of Eq (2.1) is unstable when $\tau>\tau_0$; when $\tau=\tau_0$, model (2.1) undergoes a Hopf bifurcation.

The detailed proving process of the Theorem is given in Appendix A.

3. Stability and direction of the Hopf bifurcation

We investigate the direction of Hopf bifurcation and the properties of the bifurcating periodic solutions at the positive equilibrium in this section.

Theorem 3.1. If $\mu_2>0$ ($\mu_2<0$), the model undergoes a supercritical (subcritical) Hopf bifurcation at $P^*(x_1^*,y_1^*,E_1^*)$; moreover, if $\beta_2<0$ ($\beta_2>0$) then the bifurcating periodic solutions are stable (unstable); if $T_2>0$ ($T_2<0$), the periodic of bifurcating periodic solutions increase (decrease). Here

$$\begin{aligned}c_1(0)&=\frac{i}{2\omega_{10}\tau_k}\Big(g_{20}g_{11}-2|g_{11}|^2-\frac{|g_{02}|^2}{3}\Big)+\frac{g_{21}}{2},\\\mu_2&=-\frac{Re\{c_1(0)\}}{Re\{\lambda'(\tau_k)\}},\qquad \beta_2=2Re\{c_1(0)\},\\T_2&=\frac{Im\{c_1(0)\}+\mu_2 Im\{\lambda'(\tau_k)\}}{\omega_{10}\tau_k}.\end{aligned}$$

The detailed proof of the Theorem is given in Appendix B.

4. Optimal harvesting

In order to achieve species persistence and profit maximization, optimal harvesting problem for model (1.3) without time delay is discussed in this section. We consider instantaneous annual discount rate δ, we give a continuous time stream of revenues $\mathcal{J}$ as follows

$$\mathcal{J} = \int_{t_0}^{t_f} E(p_1 q_1 P - w)e^{-\delta t} dt. \tag{4.1}$$

The control constrain on this interval $0 < E(t) < E^{max}$. Here, E^{max} stands for the maximum harvesting effort. The optimal prey and predator densities and the corresponding optimal harvesting effort are represented by $N^{optimal}$, $P^{optimal}$ and $E^{optimal}$, respectively. We are committed to calculating the optimal harvesting effort $E^{optimal}$ which satisfies the following formula

$$\mathcal{J}(E^{optimal}) = \max\{\mathcal{J}(E)|E \in U\}, \tag{4.2}$$

where U presents the control set written as

$$U = \{E \mid E \text{ is measurable and } 0 \leq E \leq E^{max} \text{ for all } t\}. \tag{4.3}$$

The calculation procedure of $N^{optimal}$, $P^{optimal}$ and $E^{optimal}$ are shown in Appendix C.

5. Numerical simulation

In this section, we will employ several specific examples to simulate the solutions to model (1.3), and verify the analytical results of the existence of Hopf bifurcation. Our analytical results illustrate that Hopf bifurcation arises in model (1.3) when the value of bifurcation parameter τ crosses critical values $\tau = \tau_k$, where

$$\tau_k = \frac{1}{\omega_{10}} \arccos \frac{(A_3 - A_1 A_4)\omega_{10}^2 - A_2 A_3}{A_3^2 + A_4^2 \omega_{10}^2} + \frac{2k\pi}{\omega_{10}}, k = 0, 1, 2, 3 \cdots,$$

and ω_{10} is the root of equation ${\omega_1}^4 + (A_1^2 - 2A_2 - A_4^2){\omega_1}^2 + (A_2^2 - A_3^2) = 0$. Here, bifurcation parameter τ is the maturation time of prey. In order to illustrate the Hopf bifurcation of (1.3). We first choose the parameter values as follows: $r = 1.01$, $K = 0.91$, $e_2 = 1.01$, $h_1 = 0.99$, $h_2 = 0.01$, $n_1 = 0.85$, $n_2 = 0.98$, $A = 0.98$, $m' = 1.99$, $q_1 = 0.91$, $p_1 = 360$, $w = 1.01$, $Q = 0.51$. The scientific significance of these parameters are shown in Table 1, under the above parameters, model (1.3) becomes the following model (5.1)

$$\begin{cases} \dfrac{dN}{dT} = 1.01N\Big(1 - \dfrac{N(t-\tau)}{0.91}\Big) - \dfrac{0.45(\frac{N}{P})}{1 + 0.45 \cdot 0.99(\frac{N}{P}) + 1.01 \cdot 0.01(\frac{0.98}{P})} P, \\ \dfrac{dP}{dT} = \dfrac{0.85 \cdot 0.45(\frac{N}{P}) + 0.98 \cdot 1.01(\frac{0.98}{P})}{1 + 0.45 \cdot 0.99(\frac{N}{P}) + 1.01 \cdot 0.01(\frac{0.98}{P})} P - 1.99P - 0.91EP, \\ E(360 \cdot 0.91P - 1.01) - 0.51 = 0. \end{cases} \tag{5.1}$$

Through maple software, we get $P_1(N^*, P^*, E^*) = (0.7191, 0.2939, 0.0054)$ and $P_1^*(x_1^*, y_1^*, E_1^*) = (0.7903, 0.7248, 0.0108)$ are respectively the equilibrium of models (5.1) and (A.2) with above parameters.

Table 1. Meaning and dimension of the parameters.

Parameter	Biological significance	Dimension
r	The intrinsic growth rate of the prey	Time^{-1}
K	Carrying capacity of the prey	Biomass
e_1	The coefficient of predator capture on prey	Time^{-1}
e_2	The coefficient of predator capture on additional food	Time^{-1}
h_1	Handing time per predator per unit of the ratio $\frac{N}{P}$ prey biomass	Time
h_2	Handing time per predator per unit of the ratio $\frac{N}{P}$ additional food biomass	Time
n_1	The nutritional value of the prey	Percent
n_2	The nutritional value of the additional food	Percent
A	The additional food for the predator	Biomass
m'	The natural mortality of the predator	Time^{-1}
q_1	The harvesting capacity coefficient	Time^{-1}
p_1	The price per unit predator biomass	–
w	The cost per unit predator harvesting efforts	–
Q	The net economic revenue	–

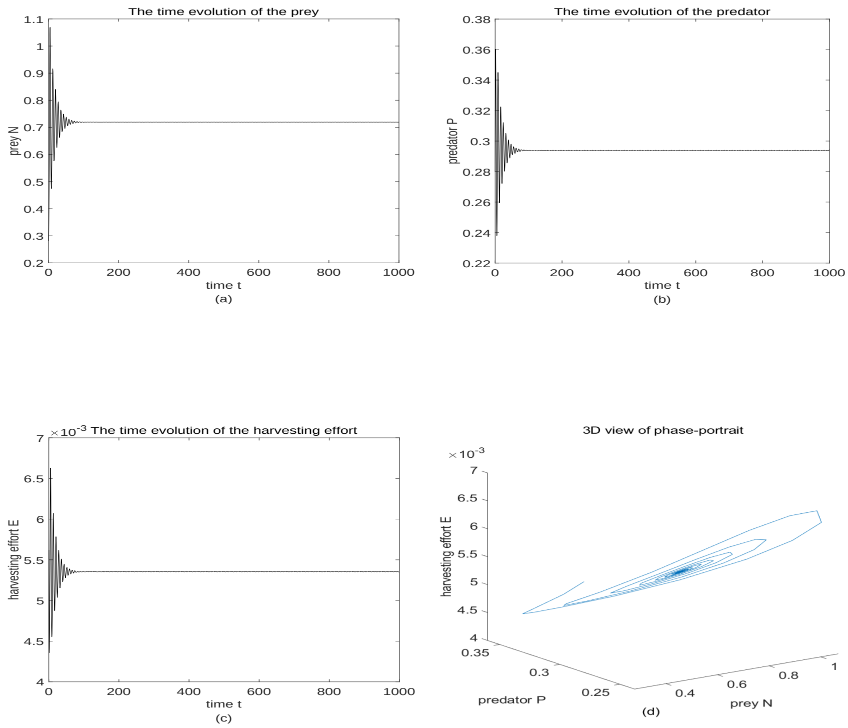

Figure 1. Numerical simulations of model (5.1) with $\tau = 1.63 < \tau_0 = 1.86$: (a) the time evolution of the prey; (b) the time evolution of the predator; (c) the time evolution of the harvesting effort of predator; (d) the phase trajectory of model (5.1). Equilibrium $P_1(N^*, P^*, E^*)$ is asymptotically stable.

Substituting the value of the positive equilibrium $P_1^*(x_1^*, y_1^*, E_1^*)$ in the expression of A_1, A_2, A_3 and A_4 to calculate the values as follows: $A_1 = 0.81$, $A_2 = -0.16$, $A_3 = 0.73$ and $A_4 = 0.79$ which surely satisfy the conditions of Theorem 2.1 (that is $A_1 + A_4 = 1.60 > 0$, $A_2 + A_3 = 0.56 > 0$ and $A_2 - A_3 = -0.89 < 0$). In addition, we further substitute A_1, A_2, A_3 and A_4 to equation (2.8) to calculate $\omega_{10} = 0.74$, then substituting ω_{10} in the expression of τ_k to yield $\tau_0 = 1.86$. A series of calculations show that $g_{20} = -12.70 + 3.11i$, $g_{11} = -4.43 - 10.67i$, $g_{02} = 11.05 - 3.71i$, $g_{21} = -106.05 + 74.57i$, $c_1(0) = -97.31 - 43.88i$, $Re\{\lambda'(\tau_k)\} = 1.01$, $Im\{\lambda'(\tau_k)\} = 2.35$, $\mu_2 = 96.35 > 0$, $\beta_2 = -194.62 < 0$, $T_2 = 134.80 > 0$. Hence, by Theorem 3.1, the periodic increase, and the direction is supercritical, and the periodic solutions are stable. By Matlab we will reveal how the model can arise Hopf bifurcation by choosing different time delays τ in the following figures.

When $\tau = 1.63 < \tau_0 = 1.86$, model (5.1) satisfies the condition of Theorem 2.1. So $P_1(N^*, P^*, E^*) = (0.7191, 0.2939, 0.0054)$ is asymptotically stable. Figure 1 reveals the time evolution and the phase trajectory of model (5.1) for $\tau = 1.63$. It is obvious that model (5.1) converges to the positive equilibrium.

When $\tau = 1.87 > \tau_0 = 1.86$, model (5.1) satisfies the condition of Theorem 2.1. So $P_1(N^*, P^*, E^*) = (0.7191, 0.2939, 0.0054)$ is unstable, i.e., a family of periodic solutions are bifurcated from $P_1(N^*, P^*, E^*)$. The periodic solutions and its stability are shown in Figure 2.

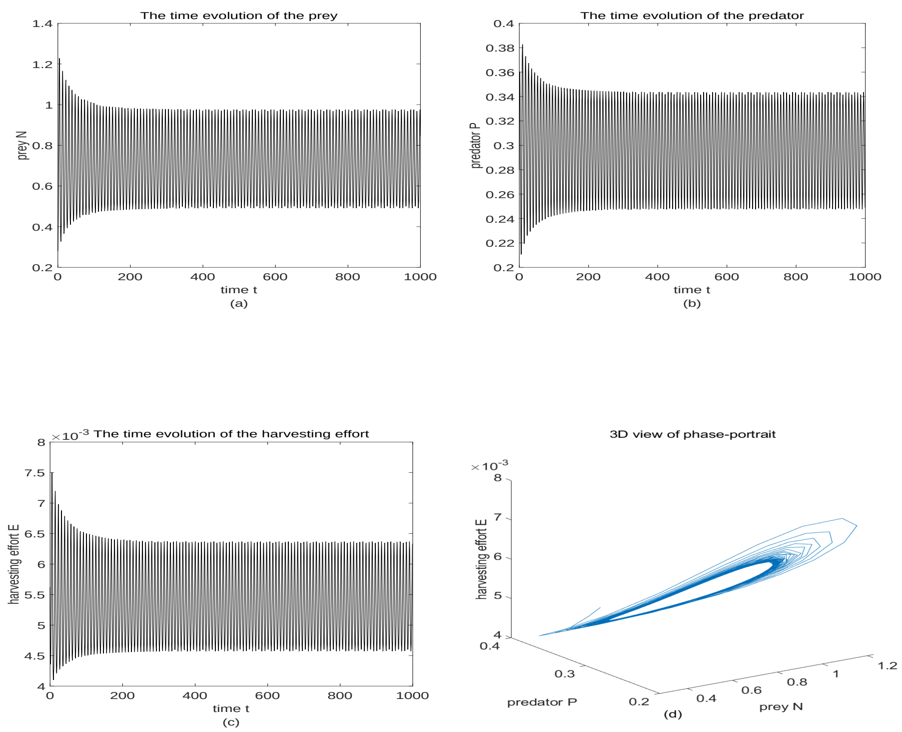

Figure 2. Numerical simulations of model (5.1) with $\tau = 1.87 > \tau_0 = 1.86$: (a) the time evolution of the prey; (b) the time evolution of the predator; (c) the time evolution of the harvesting effort of predator; (d) the phase trajectory of model (5.1). Equilibrium $P_1(N^*, P^*, E^*)$ is unstable and there exist bifurcating periodic solutions.

Combined with Figures 1 and 2, we can see that the size of maturation time τ affects the dynamic behaviors of the model, see Figure 3. This means that if time delay τ exceeds critical value, bifurcation behavior occurs at the positive equilibrium $P_1(N^*, P^*, E^*)$ of model (1.3).

We choose the parameter values as follows: $r = 0.2$, $K = 0.1$, $e_2 = 0.7$, $h_1 = 0.95$, $h_2 = 0.8$, $n_1 = 0.1$, $n_2 = 3$, $A = 0.01$, $m' = 0.9$, $q_1 = 5$, $p_1 = 1$, $w = 0.01$, $\delta = 0.01$. $(N^{optimal}, P^{optimal})$ and $E^{optimal}$ as capture rate e_1 increase are shown by (a) in Figure 4. It shows that with the increase of capture rate e_1, the optimal prey population decreases initially and increases afterwards, optimal predator population gradually decreasing, and the optimal harvesting effort gradually decreases. Besides, we choose the parameter values as follows: $r = 1$, $K = 0.45$, $e_1 = 60$, $e_2 = 0.2$, $h_1 = 1$, $h_2 = 0.02$, $n_1 = 1.5$, $n_2 = 1$, $m' = 0.01$, $q_1 = 1.44$, $p_1 = 0.02$, $w = 1.01$, $\delta = 0.1$. $(N^{optimal}, P^{optimal})$ and $E^{optimal}$ as additional food A increase are shown by (b) in Figure 4. It displays that with the increase of additional food A, the corresponding optimal prey and predator populations gradually increase, and the optimal harvesting effort gradually decreases.

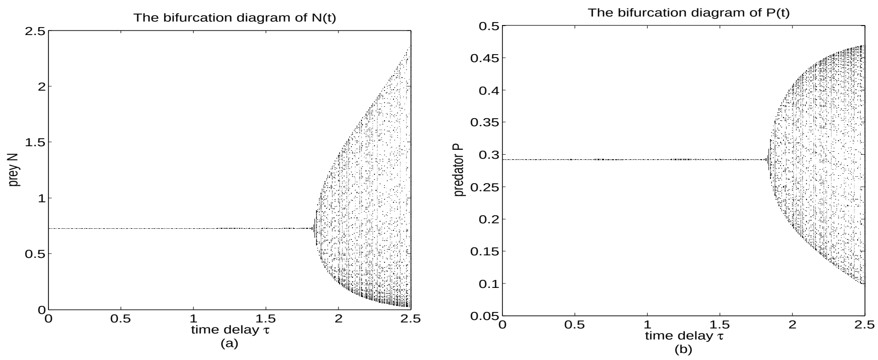

Figure 3. The bifurcation diagram of model (1.3) with respect to τ. (a) the bifurcation diagram of $N(t)$; (b) the bifurcation diagram of $P(t)$.

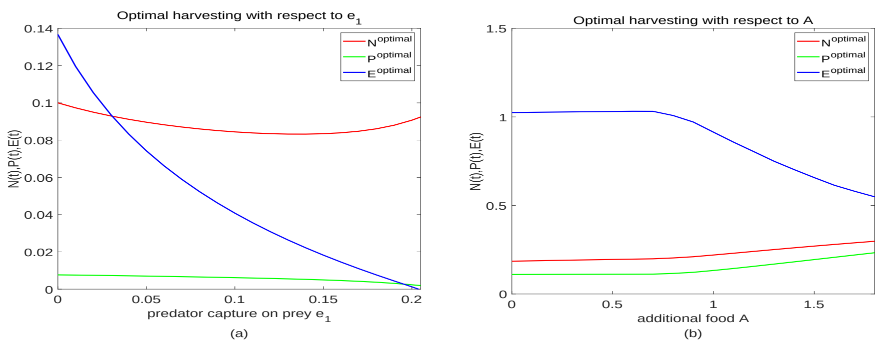

Figure 4. Optimal harvesting with respect to different parameters. (a) the coefficient of predator capture on prey $e_1 \in (0, 0.21)$; (b) additional food $A \in (0, 1.80)$.

6. Discussion and conclusions

In our paper, based on a predator-prey model with additional food proposed by Kumar et al. [29], we incorporate time delay and harvesting into the above model and establish a differential-algebraic bio-economic model. Through a series of analytical analysis we obtain the results about the existence of positive equilibrium, the conditions of steady-state and Hopf bifurcation, and the direction of bifurcation as well as the stability of bifurcating periodic solutions. Firstly, the local stability condition of positive equilibrium of model (2.1) with time delay is $A_2 - A_3 > 0$, while that without time delay are $A_1 + A_4 > 0$ and $A_2 + A_3 > 0$. Theorem 2.1 implies that the presence of the mature delay can destabilize model (2.1). When $\tau < \tau_0$, equilibrium $P_0^*(x^*, y^*, E^*)$ of model (2.1) is stable. The equilibrium is unstable when $\tau > \tau_0$; when $\tau = \tau_0$, model (2.1) has a Hopf bifurcation near the equilibrium. Besides, Theorem 3.1 displays that the direction of the bifurcation is determined by μ_2, the stability of bifurcating periodic solutions is determined by β_2, and the period of the bifurcating periodic solutions is determined by T_2. Last, optimal harvesting strategies for model (1.3) without time delay are investigated. We achieve optimal harvesting equilibrium ($N^{optimal}, P^{optimal}$) and optimal harvesting effort $E^{optimal}$.

The numerical simulation of the model is carried out through Maple and Matlab software, and we find that the results of the numerical simulation agree with the theoretical results in Theorems 2.1 and 3.1. The influence of the bifurcation parameter τ on the dynamics of prey, predator and harvesting effort is discussed. The experimental results illustrate that the positive equilibrium of the model is locally asymptotically stable when bifurcation parameter $\tau < 1.86$, see Figures 1. Conversely, equilibrium $P_1(N^*, P^*, E^*)$ is unstable and there exist bifurcating periodic solutions which are stable when bifurcation parameter $\tau > 1.86$, see Figure 2. The bifurcation diagram of (1.3) when $\tau = 1.86$ is presented in Figure 3, and the direction of bifurcation is supercritical. This also illustrates the influence of time delay τ which is one of the causes of population size fluctuation on the Hopf bifurcation of model (1.3), i.e. the presence of the mature delay can destabilize model (1.3). Furthermore, we display optimal harvesting strategies in Figure 4, and depict the change of optimal harvesting equilibrium and optimal harvesting effort with respect to the rate of predator capture on prey e_1 and extra food A, respectively. The phenomenon in Figure 4 (a) is expected due to the stronger impact of the coefficient of predator capture on prey e_1. From Figure 4 (a), we know that optimal harvesting effort approaches zero when the coefficient of predator capture on prey $e_1 = 0.21$. This means that when the coefficient of predator capture on prey e_1 is beyond the level 0.21, harvesting predators should not be considered in order to prevent extinction. Figure 4 (b) shows that the optimal harvesting effort gradually decreases, while optimal prey and predator populations gradually increase, since additional food A distracts the predator from attacking the prey. At the same time, in order to prevent harmful prey from growing to uncontrollable numbers, the harvesting effort on predator should be reduced.

There are many topics that require us to refine and further analyze our model. On the one hand, the discrete time delay is considered in this study of Hopf bifurcation while more rich dynamic behaviors are generated by incorporating the distributed delays. On the other hand, the influence of random factors could not be ignored in which we introduce white noise into our model which involving the multiplicative random excitation and additive random excitation to analyze the stochastic P-bifurcation and stochastic D-bifurcation. The model is displayed as follows

$$\begin{cases} \dfrac{dN}{dT} = rN\Big(1 - \dfrac{N}{K}\Big) - \dfrac{e_1(\frac{N}{P})}{1 + e_1h_1(\frac{N}{P}) + e_2h_2(\frac{A}{P})}P + \alpha_1 N\xi(t) + \eta_1\eta(t), \\ \dfrac{dP}{dT} = \dfrac{n_1e_1(\frac{N}{P}) + n_2e_2(\frac{A}{P})}{1 + e_1h_1(\frac{N}{P}) + e_2h_2(\frac{A}{P})}P - m'P - q_1EP + \alpha_2 P\xi(t) + \eta_2\eta(t), \\ E(p_1q_1P - w) - Q = 0, \end{cases}$$

where $\xi(t), \eta(t)$ represent the multiplicative random excitation and additive random excitation respectively. The above mentions make our model more interesting and complicated and remain to be done in the future.

Use of AI tools declaration

The authors declare they have not used Artificial Intelligence (AI) tools in the creation of this article.

Acknowledgments

The authors thank the editor and referees for their careful reading and valuable comments. The work is supported by the National Natural Science Foundation of China (No.12101211) and the Program for Innovative Research Team of the Higher Education Institution of Hubei Province (No.T201812) and the Scientific Research Project of Education Department of Hubei Province (No.B2020090) and the Program of Graduate Education Innovation of Hubei Minzu University (No.MYK2023042).

Conflict of interest

The authors declare that there is no conflict of interest.

References

1. A. J. Lotka, *Elements of Physical Biology*, Williams and Wilkins, Baltimore, 1925.
2. V. Volterra, Variations and fluctuations of the number of individuals in animal species living together, *J. Cons. Perm. Int. Ent. Mer.*, **3** (1928), 3–51. https://doi.org/10.1093/icesjms/3.1.3
3. R. S. Cantrell, C. Cosner, On the dynamics of predator-prey models with the Beddington-DeAngelis functional response, *J. Math. Anal. Appl.*, **257** (2001), 206–222. https://doi.org/10.1006/jmaa.2000.7343
4. D. M. Xiao, S. G. Ruan, Codimension two bifurcations in a predator-prey system with group defense, *Int. J. Bifurcat. Chaos.*, **11** (2001), 2123–2131. https://doi.org/10.1142/S021812740100336X
5. T. K. Kar, S. Misra, Influence of prey reserve in a prey-predator fishery, *Nonlinear Anal.*, **65** (2006), 1725–1735. https://doi.org/10.1016/j.na.2005.11.049
6. A. A. Elsadany, A. E. Matouk, Dynamical behaviors of fractional-order Lotka-Volterra predator-prey model and its discretization, *J. Appl. Math. Comput.*, **49** (2015), 269–283. https://doi.org/10.1007/s12190-014-0838-6

7. C. S. Holling, The components of predation as revealed by a study of small-mammal predation of the European Pine Sawfly, *Can. Ent.*, **91** (1959), 293–320. https://doi.org/10.4039/Ent91293-5
8. C. S. Holling, The functional response of predators to prey density and its role in mimicry and population regulation, *Mem. Entomol. Soc. Can.*, **97** (1965), 5–60. https://doi.org/10.4039/entm9745fv
9. C. S. Holling, The functional response of invertebrate predators to prey density, *Mem. Entomol. Soc. Can.*, **98** (1966), 5–86. https://doi.org/10.4039/entm9848fv
10. R. E. Kooij, A. Zegeling, Qualitative properties of two-dimensional predator-prey systems, *Nonlinear Anal.*, **29** (1997), 693–715. https://doi.org/10.1016/S0362-546X(96)00068-5
11. M. Hesaaraki, S. M. Moghadas, Existence of limit cycles for predator-prey systems with a class of functional responses, *Ecol. Modell.*, **142** (2001), 1–9. https://doi.org/10.1016/S0304-3800(00)00442-7
12. H. Wang, C. H. Zhang, Dynamics of a predator-prey reaction-diffusion system with non-monotonic functional response function, *Ann. Appl. Math.*, **34** (2018), 199–220.
13. D. L. De Angelis, R. A. Goldstein, R. V. O'Neill, A model for tropic interactions, *Ecology*, **56** (1975), 881–892. https://doi.org/10.2307/1936298
14. L. R. Ginzburg, H. R. Akcakaya, Consequences of ratio-dependent predation for steady-state properties of ecosystems, *Ecology*, **73** (1992), 1536–1543. https://doi.org/10.2307/1940006
15. A. P. Gutierrez, Physiological basis of ratio-dependent predator-prey theory: the metabolic pool model as a paradigm, *Ecology*, **73** (1992), 1552–1563. https://doi.org/10.2307/1940008
16. H. R. Akcakaya, R. Arditi, L. R. Ginzburg, Ratio-dependent prediction: An abstraction that works, *Ecology*, **76** (1995), 995–1004. https://doi.org/10.2307/1939362
17. A. A. Berryman, The origins and evolutions of predator-prey theory, *Ecology*, **73** (1992), 1530–1535. https://doi.org/10.2307/1940005
18. M. Haque, Ratio-dependent predator-prey models of interacting populations, *Bull. Math. Biol.*, **71** (2009), 430–452. https://doi.org/10.1007/s11538-008-9368-4
19. D. Kesh, A. K. Sarkar, A. B. Roy, Persistence of two prey-one predator system with ratio-dependent predator influence, *Math. Meth. Appl. Sci.*, **23** (2000), 347–356.
20. R. Xu, L. S. Chen, Persistence and stability for a two-species ratio-dependent predator-prey system with time delay in a two-patch environment, *Comput. Math. Appl.*, **40** (2000), 577–588. https://doi.org/10.1016/S0898-1221(00)00181-4
21. S. Y. Tang, L. S. Chen, Global qualitative analysis for a ratio-dependent predator-prey model with delay, *J. Math. Anal. Appl.*, **266** (2002), 401–419. https://doi.org/10.1006/jmaa.2001.7751
22. Y. H. Fan, W. T. Li, Permanence for a delayed discrete ratio-dependent predator-prey system with Holling type functional response, *J. Math. Anal. Appl.*, **299** (2004), 357–374. https://doi.org/10.1016/j.jmaa.2004.02.061
23. P. D. N. Srinivasu, B. Prasad, Role of quantity of additional food to predators as a control in predator-prey systems with relevance to pest management and biological conservation, *Bull. Math. Biol.*, **73** (2011), 2249–2276. https://doi.org/10.1007/s11538-010-9601-9
24. A. Basheer, E. Quansah, R. D. Parshad, The effect of additional food in Holling Tanner type models, *Int. J. Dyn. Control*, **7** (2019), 1195–1212. https://doi.org/10.1007/s40435-019-00580-3

25. S. Samaddar, M. Dhar, P. Bhattacharya, Effect of fear on prey-predator dynamics: Exploring the role of prey refuge and additional food, *Chaos*, **30** (2020), 063129. https://doi.org/10.1063/5.0006968

26. L. Y. Wu, H. Zheng, Hopf bifurcation in a delayed predator-prey system with asymmetric functional response and additional food, *AIMS Math.*, **6** (2021), 12225–12244. https://doi.org/10.3934/math.2021708

27. R. Arditi, L. R. Ginzburg, Coupling in predator-prey dynamics: ratio-dependence, *J. Theor. Biol.*, **139** (1989), 311–326. https://doi.org/10.1016/S0022-5193(89)80211-5

28. P. N. D. Srinivasu, B. Prasad, M. Venkatesulu, Biological control through provision of additional food to predators: a theoretical study, *Theor. Popul. Biol.*, **72** (2007), 111–120. https://doi.org/10.1016/j.tpb.2007.03.011

29. D. Kumar, S. P. Chakrabarty, A predator-prey model with additional food supply to predators: dynamics and applications, *J. Comp. Appl. Math.*, **37** (2018), 763–784. https://doi.org/10.1007/s40314-016-0369-x

30. Z. J. Liu, R. H. Tan, L. S. Chen, Global stability in a periodic delayed predator-prey system, *Appl. Math. Comput.*, **186** (2007), 389–403. https://doi.org/10.1016/j.amc.2006.07.123

31. X. S. Liu, B. X. Dai, Dynamics of a generalized predator-prey model with delay and impulse via the basic reproduction number, *Math. Meth. Appl. Sci.*, **42** (2019), 6878–6895. https://doi.org/10.1002/mma.5794

32. S. Y. Li, Hopf bifurcation, stability switches and chaos in a prey-predator system with three stage structure and two time delays, *Math. Biosci. Eng.*, **16** (2019), 6934–6961. https://doi.org/10.3934/mbe.2019348

33. K. Manna, M. Banerjee, Stability of Hopf-bifurcating limit cycles in a diffusion-driven prey-predator system with Allee effect and time delay, *Math. Biosci. Eng.*, **16** (2019), 2411–2446. https://doi.org/10.3934/mbe.2019121

34. X. Jiang, R. Zhang, Z. K. She, Dynamics of a diffusive predator-prey system with ratio-dependent functional response and time delay, *Int. J. Biomath.*, **13** (2020), 2050036. https://doi.org/10.1142/S1793524520500369

35. Q. F. Tang, G. H. Zhang, Stability and Hopf bifurcations in a competitive tumour-immune system with intrinsic recruitment delay and chemotherapy, *Math. Biosci. Eng.*, **18** (2021), 1941–1965. https://doi.org/10.3934/mbe.2021101

36. T. K. Kar, S. Misra, B. Mukhopadhyay, A bioeconomic model of a ratio-dependent predator-prey system and optimal harvesting, *J. Appl. Math. Comput.*, **22** (2006), 387–401. https://doi.org/10.1007/BF02896487

37. H. Y. Zhao, X. X. Huang, X. B. Zhang, Hopf bifurcation and harvesting control of a bioeconomic plankton model with delay and diffusion terms, *Phys. A.*, **421** (2015), 300–315. https://doi.org/10.1016/j.physa.2014.11.042

38. X. Zhang, Q. L. Zhang, C. Liu, Z. Y. Xiang, Bifurcations of a singular prey-predator economic model with time delay and stage structure, *Chaos Soliton. Fractals*, **42** (2009), 1485–1494. https://doi.org/10.1016/j.chaos.2009.03.051

39. G. D. Zhang, L. L. Zhu, B. S. Chen, Hopf bifurcation and stability for a differential-algebraic biological economic system, *Appl. Math. Comput.*, **217** (2010), 330–338. https://doi.org/10.1016/j.amc.2010.05.065

40. K. Chakraborty, M. Chakraborty, T. K. Kar, Bifurcation and control of a bioeconomic model of a prey-predator system with a time delay, *Nonlinear Anal-Hybrid.*, **5** (2011), 613–625. https://doi.org/10.1016/j.nahs.2011.05.004

41. B. S. Chen, J. J. Chen, Bifurcation and chaotic behavior of a discrete singular biological economic system, *Appl. Math. Comput.*, **219** (2012), 2371–2386. https://doi.org/10.1016/j.amc.2012.07.043

42. D. Pal, G. S. Mahaptra, G. P. Samanta, Optimal harvesting of prey-predator system with interval biological parameters: a bioeconomic model, *Math. Biosci.*, **241** (2013), 181–187. https://doi.org/10.1016/j.mbs.2012.11.007

43. Y. Zhang, Q. L. Zhang, X. G. Yan, Complex dynamics in a singular Leslie-Gower predator-prey bioeconomic model with time delay and stochastic fluctuations, *Phys. A.*, **404** (2014), 180–191. https://doi.org/10.1016/j.physa.2014.02.013

44. X. Zhang, S. N. Song, J. H. Wu, Oscillations, fluctuation intensity and optimal harvesting of a bio-economic model in a complex habitat, *J. Math. Anal. Appl.*, **436** (2016), 692–717. https://doi.org/10.1016/j.jmaa.2015.11.068

45. C. W. Clark, Mathematical Bioeconomics: The Optimal Management of Renewable Resources, Wiley, New York, 1976. https://doi.org/10.1137/1020117

46. C. H. Katz, A nonequilibrium marine predator-prey interaction, *Ecology*, **66** (1985), 1426–1438. https://doi.org/10.2307/1938005

47. W. Stephen, Introduction to Applied Nonlinear Dynamical Systems and Chaos, Springer, New York, 2003. https://doi.org/10.1063/1.4822950

48. Q. Tang, G. Zhang, Stability and Hopf bifurcations in a competitive tumour-immune system with intrinsic recruitment delay and chemotherapy, *Math. Biosci. Eng.*, **18** (2021), 1941–1965. https://doi.org/10.3934/mbe.2021101

49. K. L. Cooke, Z. Grossman, Discrete delay, distributed delay and stability switches, *J. Math. Anal. Appl.*, **86** (1982), 592–627. https://doi.org/10.1016/0022-247X(82)90243-8

Appendix A

In order to linearize model (2.1), we consider the following linear transformation

$$\begin{pmatrix} x \\ y \\ E \end{pmatrix} = \begin{pmatrix} 1 & 0 & 0 \\ 0 & 1 & 0 \\ 0 & -\frac{pqE^*}{pqy^*-w} & 1 \end{pmatrix} \begin{pmatrix} x_1 \\ y_1 \\ E_1 \end{pmatrix}.$$

Thus model (2.1) could be rewritten as

$$\begin{cases} \dfrac{dx_1}{dt} = x_1(1 - x_1(t-\tau)) - \dfrac{cx_1y_1}{x_1 + y_1 + \alpha\xi}, \\ \dfrac{dy_1}{dt} = \dfrac{b(x_1+\xi)y_1}{x_1 + y_1 + \alpha\xi} - my_1 - q\Big(E_1 - \dfrac{pqE^*y_1}{pqy^* - w}\Big)y_1, \\ \Big(E_1 - \dfrac{pqE^*y_1}{pqy^* - w}\Big)(pqy_1 - w) - Q = 0. \end{cases} \tag{A.2}$$

The internal equilibrium of the model (A.2) becomes $P_1^*(x_1^*, y_1^*, E_1^*)$, we transform the equilibrium into zero by linear transformation $x_1 = x_1^* + x_2$, $y_1 = y_1^* + y_2$, $E_1 = E_1^* + I(x_2, y_2)$, where

$$I(x_2, y_2) = \frac{pqE^*(y_1^* + y_2)}{pqy_1^* - w} + \frac{Q}{pq(y_1^* + y_2) - w} - \frac{pqE^*y_1^*}{pqy_1^* - w} - E^*.$$

Model (A.2) is expressed as the following equation according to the above transformations

$$\begin{cases} \dfrac{dx_2}{dt} = (x_1^* + x_2)((1 - (x_1^* + x_2(t-\tau))) - \dfrac{c(x_1^* + x_2)(y_1^* + y_2)}{x_1^* + x_2 + y_1^* + y_2 + \alpha\xi}, \\ \dfrac{dy_2}{dt} = (y_1^* + y_2)\Big(\dfrac{b(x_1^* + x_2 + \xi)}{x_1^* + x_2 + y_1^* + y_2 + \alpha\xi} - m - qE_1^* - qI + \dfrac{pq^2E^*(y_1^* + y_2)}{pqy^* - w}\Big). \end{cases} \tag{A.3}$$

By calculation, the Jacobian matrix of the model (A.3) at $(0, 0)$ is represented as follows

$$J = \begin{pmatrix} -x_1^*e^{-\lambda\tau} + \dfrac{cx_1^*y_1^*}{(x_1^* + y_1^* + \alpha\xi)^2} & -\dfrac{cx_1^*(x_1^* + \alpha\xi)}{(x_1^* + y_1^* + \alpha\xi)^2} \\ \dfrac{by_1^*(y_1^* + \alpha\xi - \xi)}{(x_1^* + y_1^* + \alpha\xi)^2} & -\dfrac{b(x_1^* + \xi)y_1^*}{(x_1^* + y_1^* + \alpha\xi)^2} + \dfrac{pq^2E^*y_1^*}{pqy_1^* - w} \end{pmatrix}.$$

The formula for the determination of the characteristic equation gives that $\lambda^2 + A_1\lambda + A_2 + (A_3 + A_4\lambda)e^{-\lambda\tau} = 0$, where

$$\begin{aligned} A_1 &= \frac{b(x_1^* + \xi)y_1^*}{(x_1^* + y_1^* + \alpha\xi)^2} - \frac{pq^2E^*y_1^*}{pqy_1^* - w} - \frac{cx_1^*y_1^*}{(x_1^* + y_1^* + \alpha\xi)^2}, \\ A_2 &= -\frac{cbx_1^*{y_1^*}^2(x_1^* + \xi)}{(x_1^* + y_1^* + \alpha\xi)^4} + \frac{pq^2cx_1^*{y_1^*}^2E^*}{(x_1^* + y_1^* + \alpha\xi)^2(pqy_1^* - w)} + \frac{bcx_1^*y_1^*(x_1^* + \alpha\xi)(y_1^* + \alpha\xi - \xi)}{(x_1^* + y_1^* + \alpha\xi)^4}, \\ A_3 &= \frac{bx_1^*y_1^*(x_1^* + \xi)}{(x_1^* + y_1^* + \alpha\xi)^2} - \frac{x_1^*y_1^*pq^2E^*}{pqy_1^* - w}, \\ A_4 &= x_1^*. \end{aligned}$$

When $\tau = 0$, the characteristic equation is as follows

$$\lambda^2 + (A_1 + A_4)\lambda + A_2 + A_3 = 0. \tag{A.4}$$

By Routh-Hurwitz criterion, we know that $P_1^*(x_1^*, y_1^*, E_1^*)$ is locally asymptotically stable provided that the conditions $A_1 + A_4 > 0$ and $A_2 + A_3 > 0$.

When $\tau > 0$, the characteristic equation is yielded to

$$\lambda^2 + A_1\lambda + A_2 + (A_3 + A_4\lambda)e^{-\lambda\tau} = 0. \tag{A.5}$$

Suppose that $i\omega_1$ is a solution of (A.5), one gets

$$-{\omega_1}^2 + A_1 i\omega_1 + A_2 + (A_3 + A_4 i\omega_1)e^{-i\omega_1\tau} = 0. \tag{A.6}$$

Separating the real and imaginary parts of Eq (A.6), we obtain

$$A_4\omega_1 \sin\omega_1\tau + A_3\cos\omega_1\tau = \omega_1^2 - A_2, \ \ A_4\omega_1\cos\omega_1\tau - A_3\sin\omega_1\tau = -A_1\omega_1. \tag{A.7}$$

Furthermore,

$${\omega_1}^4 + (A_1^2 - 2A_2 - A_4^2){\omega_1}^2 + (A_2^2 - A_3^2) = 0. \tag{A.8}$$

Let $u = \omega_1^2$. Then, Eq (A.8) becomes

$$f(u) = u^2 + (A_1^2 - 2A_2 - A_4^2)u + (A_2^2 - A_3^2) = 0.$$

If $A_1 > 0, A_3 > 0, A_2 + A_3 > 0$ and $A_2 - A_3 < 0$, then Eq (A.8) exists a unique positive real root ω_{10}, hence (A.5) has a pair of pure imaginary roots $\pm i\omega_{10}$ at the critical value $\tau_k > 0$, which could be denoted as

$$\tau_k = \frac{1}{\omega_{10}} \arccos \frac{(A_3 - A_1A_4)\omega_{10}^2 - A_2A_3}{A_3^2 + A_4^2\omega_{10}^2} + \frac{2k\pi}{\omega_{10}}, k = 0, 1, 2, 3 \cdots . \tag{A.9}$$

If $A_2 - A_3 > 0$, (A.5) has no real roots and $P_1^*(x_1^*, y_1^*, E_1^*)$ is asymptotical stability for any $\tau > 0$.

We have to prove that $\frac{d}{d\tau}Re\lambda(\tau_k) > 0$ is true for guaranteeing the existence of Hopf bifurcation. Consider the following equation

$$\Big(\frac{d\lambda}{d\tau}\Big)^{-1} = \frac{2\lambda + A_1 + (-A_3\tau + A_4 - A_4\tau\lambda)e^{-\lambda\tau}}{(A_3\lambda + A_4\lambda^2)e^{-\lambda\tau}}. \tag{A.10}$$

Using a computation process similar to that of Tang [48] and Cooke [49], one yields

$$\begin{aligned}
&\text{Sign}\Big\{\tfrac{d}{d\tau}Re\lambda\Big\}_{\lambda=i\omega_{10}} = \text{Sign}\Big\{Re\Big(\tfrac{d\lambda}{d\tau}\Big)^{-1}\Big\}_{\lambda=i\omega_{10}} \\
&= \text{Sign}\left\{Re\left[\frac{(2i\omega_{10} + A_1)(\cos(\omega_{10}\tau) + i\sin(\omega_{10}\tau)) - A_3\tau + A_4 - A_4\tau i\omega_{10}}{A_3 i\omega_{10} - A_4\omega_{10}^2}\right]\right\} \\
&= \text{Sign}\left\{\frac{2A_3w_{10}^2cos(w_{10}\tau) + 2A_4w_{10}^3sin(w_{10}\tau) - A_1A_4w_{10}^2cos(w_{10}\tau) + A_1A_3w_{10}sin(w_{10}\tau) - A_4^2w_{10}^2}{A_3^2\omega_{10}^2 + A_4^2\omega_{10}^4}\right\} \\
&= \text{Sign}\left\{\frac{\omega_{10}^2(2\omega_{10}^2 + (A_1^2 - 2A_2 - A_4^2))}{A_3^2\omega_{10}^2 + A_4^2\omega_{10}^4}\right\} \\
&= \text{Sign}\left\{\frac{f'(\omega_{10}^2)}{A_3^2 + A_4^2\omega_{10}^2}\right\}.
\end{aligned}$$

Since $A_2 + A_3 > 0$ and $A_2 - A_3 < 0$, we know that $f(u)$ has a unique positive real root $u_0 = \omega_{10}^2$. In addition it can be shown that $f'(u_0) > 0$ (that is $f'(\omega_{10}^2) > 0$). Combined with the above analysis, we have the following theorem.

Appendix B

Let $u_1(t) = x_2(\tau t)$, $u_2(t) = y_2(\tau t)$, $\tau = \tau_k + \mu$ ($\mu \in \mathbb{R}$), then, $\mu = 0$ is the Hopf bifurcation value. The functional differential equation is considered as follows

$$u'(t) = L_\mu(u_t) + F(\mu, u_t), \tag{B.1}$$

where $u(t) = (u_1(t), u_2(t)) \in \mathbb{R}^2$ and $L_\mu : C \to \mathbb{R}^2, F : \mathbb{R} \times C \to \mathbb{R}^2$. Let us define

$$L_\mu \phi = (\tau_k + \mu) \begin{pmatrix} \frac{cx_1^* y_1^*}{(x_1^* + y_1^* + \alpha\xi)^2} & -\frac{cx_1^*(x_1^* + \alpha\xi)}{(x_1^* + y_1^* + \alpha\xi)^2} \\ \frac{by_1^*(y_1^* + \alpha\xi - \xi)}{(x_1^* + y_1^* + \alpha\xi)^2} & -\frac{b(x_1^* + \xi)y_1^*}{(x_1^* + y_1^* + \alpha\xi)^2} + \frac{pq^2 E^* y_1^*}{pqy_1^* - w} \end{pmatrix} \phi(0) + (\tau_k + \mu) \begin{pmatrix} -x_1^* & 0 \\ 0 & 0 \end{pmatrix} \phi(-1) \tag{B.2}$$

and

$$F(\mu, \phi) = (\tau_k + \mu) \begin{pmatrix} F_1 \\ F_2 \end{pmatrix}, \tag{B.3}$$

where

$$\begin{aligned} F_1 =& \Big(\frac{cy_1^*}{\mu_1^2} - \frac{cx_1^* y_1^*}{\mu_1^3}\Big)\phi_1^2(0) - \phi_1^2(-1) + \Big(\frac{cx_1^*}{\mu_1^2} - \frac{cx_1^* y_1^*}{\mu_1^3}\Big)\phi_2^2(0) - \Big(\frac{c\alpha\xi}{\mu_1^2} + \frac{2cx_1^* y_1^*}{\mu_1^3}\Big)\phi_1(0)\phi_2(0) \\ &+ \Big(-\frac{c(x_1^* - \alpha\xi)}{\mu_1^3} + \frac{3cx_1^* y_1^*}{\mu_1^4}\Big)\phi_1(0)\phi_2^2(0) + \Big(-\frac{c(y_1^* - \alpha\xi)}{\mu_1^3} + \frac{3cx_1^* y_1^*}{\mu_1^4}\Big)\phi_1^2(0)\phi_2(0) \\ &+ \Big(-\frac{cy_1^*}{\mu_1^3} + \frac{cx_1^* y_1^*}{\mu_1^4}\Big)\phi_1^3(0) + \Big(-\frac{cx_1^*}{\mu_1^3} + \frac{cx_1^* y_1^*}{\mu_1^4}\Big)\phi_2^3(0) + \cdots, \\ F_2 =& \Big(-\frac{by_1^*}{\mu_1^2} + \frac{b(x_1^* + \xi)y_1^*}{\mu_1^3}\Big)\phi_1^2(0) - \Big(\frac{b(x_1^* + \xi)(x_1^* + \alpha\xi)}{\mu_1^3} + \frac{pq^2 Qw}{\nu_1^3}\Big)\phi_2^2(0) \\ &+ \Big(\frac{b(\alpha\xi - \xi)}{\mu_1^2} + \frac{2b(x_1^* + \xi)y_1^*}{\mu_1^3}\Big)\phi_1(0)\phi_2(0) + \Big(\frac{b(x_1^* - \alpha\xi + 2\xi)}{\mu_1^3} - \frac{3b(x_1^* + \xi)y_1^*}{\mu_1^4}\Big)\phi_1(0)\phi_2^2(0) \\ &+ \Big(\frac{b(y_1^* - \alpha\xi + \xi)}{\mu_1^3} - \frac{3b(x_1^* + \xi)y_1^*}{\mu_1^4}\Big)\phi_1^2(0)\phi_2(0) + \Big(\frac{by_1^*}{\mu_1^3} - \frac{b(x_1^* + \xi)y_1^*}{\mu_1^4}\Big)\phi_1^3(0) \\ &+ \Big(\frac{b(x_1^* + \xi)(x_1^* + \alpha\xi)}{\mu_1^4} + \frac{p^2 q^3 Qw}{\nu_1^4}\Big)\phi_2^3(0) + \cdots, \end{aligned} \tag{B.4}$$

in which $\mu_1 = (x_1^* + y_1^* + \alpha\xi)$, $\nu_1 = (pqy_1^* - w)$ and $\phi(\theta) = (\phi_1(\theta), \phi_2(\theta)) \in C$.

There exists a 2×2 matrix function $\eta(\theta, \mu)$ $(\theta \in [-1, 0])$ such that

$$L_\mu \phi = \int_{-1}^{0} d\eta(\theta, \mu)\phi(\theta), \phi \in C. \tag{B.5}$$

At this point, bounded variation function could be chosen as

$$\eta(\theta, \mu) = (\tau_k + \mu) \begin{pmatrix} \frac{cx_1^* y_1^*}{(x_1^* + y_1^* + \alpha\xi)^2} & -\frac{cx_1^*(x_1^* + \alpha\xi)}{(x_1^* + y_1^* + \alpha\xi)^2} \\ \frac{by_1^*(y_1^* + \alpha\xi - \xi)}{(x_1^* + y_1^* + \alpha\xi)^2} & -\frac{b(x_1^* + \xi)y_1^*}{(x_1^* + y_1^* + \alpha\xi)^2} + \frac{pq^2 E^* y_1^*}{pqy_1^* - w} \end{pmatrix} \delta(\theta) - (\tau_k + \mu) \begin{pmatrix} -x_1^* & 0 \\ 0 & 0 \end{pmatrix} \delta(\theta + 1). \tag{B.6}$$

Here, $\delta(\theta)$ is the Dirac function.

For $\phi \in C^1([-1,0],\mathbb{R}^2)$, we define

$$\mathcal{A}(\mu)\phi(\theta) = \begin{cases} \dfrac{d\phi(\theta)}{d\theta}, & \theta \in [-1,0), \\ \int_{-1}^{0} d\eta(\theta,\mu)\phi(\theta), & \theta = 0, \end{cases} \tag{B.7}$$

$$R(\mu)\phi = \begin{cases} 0, & \theta \in [-1,0), \\ F(\mu,\phi), & \theta = 0. \end{cases} \tag{B.8}$$

Then, Eq (B.1) is equivalent to the following equation

$$u_t' = \mathcal{A}(\mu)u_t + R(\mu)u_t, \quad u_t(\theta) = u(t+\theta), \quad \theta \in [-1,0]. \tag{B.9}$$

The bifurcating periodic solution $u(t,\mu)$ of Eq (B.1) is affected by parameter ε, solution $u(t,\mu(\varepsilon))$ of Eq (B.1) exists amplitude $o(\varepsilon)$, nonzero exponential $\beta(\varepsilon)$ ($\beta(0) = 0$) and period $T(\varepsilon)$. Under the above assumptions, μ, T, and β have the following expansion form

$$\begin{cases} \mu = \mu_2\varepsilon^2 + \mu_4\varepsilon^4 + \cdots, \\ T = \dfrac{2\pi}{\omega}(1 + T_2\varepsilon^2 + T_4\varepsilon^4 \cdots), \\ \beta = \beta_2\varepsilon^2 + \beta_4\varepsilon^4 \cdots. \end{cases} \tag{B.10}$$

Next, we compute the coefficients μ_2, T_2, β_2. For $\psi \in C^1([0,1],(\mathbb{R}^2)^*)$, assign the conjugate operator $\mathcal{A}^*$ of $\mathcal{A}$ is as follows

$$\mathcal{A}^*\psi = \begin{cases} -\dfrac{d\psi(s)}{ds}, & s \in (0,1], \\ \int_{-1}^{0} d\eta^T(t,0)\psi(-t), & s = 0, \end{cases} \tag{B.11}$$

the adjoint bilinear form is given by

$$\langle\psi(s),\phi(\theta)\rangle = \bar{\psi}^T(0)\phi(0) - \int_{-1}^{0}\int_{\xi=0}^{\theta} \bar{\psi}^T(\xi-\theta)d\eta(\theta)\phi(\xi)d\xi, \quad \eta(\theta) = \eta(\theta,0). \tag{B.12}$$

Obviously, $\pm i\omega_{10}\tau_k$ are both eigenvalues of $\mathcal{A}(0)$ and $\mathcal{A}^*$. Now we calculate the eigenvector of $\mathcal{A}(0)$ corresponding to $i\omega_{10}\tau_k$. Let $q(\theta) = (1,\Delta)^T e^{i\omega_{10}\tau_k\theta}$, then, $\mathcal{A}(0)q(\theta) = i\omega_{10}\tau_k q(\theta)$. Combining Eq (B.6) and the definition of $\mathcal{A}(0)$, it is easy to get

$$\begin{pmatrix} -x_1^* e^{-i\omega_{10}\tau_k} + \dfrac{cx_1^*y_1^*}{\mu_1^2} & -\dfrac{cx_1^*(x_1^*+\alpha\xi)}{\mu_1^2} \\ \dfrac{by_1^*(y_1^*+\alpha\xi-\xi)}{\mu_1^2} & -\dfrac{b(x_1^*+\xi)y_1^*}{\mu_1^2} + \dfrac{pq^2E^*y_1^*}{\nu_1} \end{pmatrix} q(0) = i\omega_{10}q(0), \tag{B.13}$$

we further obtain

$$\Delta = -\left(i\omega_{10} + x_1^* e^{-i\omega_{10}\tau_k}\right)\frac{\mu_1^2}{cx_1^*(x_1^*+\alpha\xi)} + \frac{y_1^*}{x_1^*+\alpha\xi}. \tag{B.14}$$

By a similar argument as that in the above part, the eigenvector of $\mathcal{A}^*$ corresponding to $-i\omega_{10}\tau_k$ could be achieved. Let $q^*(s) = \mathcal{D}(1,\Delta^*)e^{i\omega_{10}\tau_k s}$, we also have

$$\Delta^* = \left(-i\omega_{10} + x_1^* e^{-i\omega_{10}\tau_k}\right)\frac{\mu_1^2}{by_1^*(y_1^*+\alpha\xi-\xi)} - \frac{cx_1^*}{b(y_1^*+\alpha\xi-\xi)}. \tag{B.15}$$

From Eq (B.12) one gets

$$\begin{aligned}\langle q^*(s), q(\theta)\rangle =&\bar{\mathcal{D}}(1,\bar{\Delta^*})(1,\Delta)^T - \int_{-1}^{0}\int_{\xi=0}^{\theta}\bar{\mathcal{D}}(1,\bar{\Delta^*})e^{-i\omega_{10}\tau_k(\xi-\theta)}d\eta(\theta)(1,\Delta)^T e^{i\omega_{10}\tau_k\xi}d\xi\\ =&\bar{\mathcal{D}}(1+\bar{\Delta^*}\Delta) - \bar{\mathcal{D}}\int_{-1}^{0}\int_{\xi=0}^{\theta}(1,\bar{\Delta^*})e^{i\omega_{10}\tau_k\theta}d\eta(\theta)(1,\Delta)^T d\xi\\ =&\bar{\mathcal{D}}(1+\bar{\Delta^*}\Delta) - \bar{\mathcal{D}}\int_{-1}^{0}(1,\bar{\Delta^*})\theta e^{i\omega_{10}\tau_k\theta}d\eta(\theta)(1,\Delta)^T\\ =&\bar{\mathcal{D}}\left(1+\bar{\Delta^*}\Delta + (1,\bar{\Delta^*})\tau_k\begin{pmatrix} x_1^* & 0\\ 0 & 0\end{pmatrix}e^{-i\omega_{10}\tau_k}\begin{pmatrix}1\\ \Delta\end{pmatrix}\right)\\ =&\bar{\mathcal{D}}(1+\bar{\Delta^*}\Delta + \tau_k e^{-i\omega_{10}\tau_k}x_1^*).\end{aligned} \tag{B.16}$$

Hence,

$$\mathcal{D} = \frac{1}{1+\bar{\Delta}^*\Delta\tau_k + e^{i\omega_{10}\tau_k}x_1^*},\ \ \bar{\mathcal{D}} = \frac{1}{1+\Delta^*\bar{\Delta}\tau_k + e^{-i\omega_{10}\tau_k}x_1^*}. \tag{B.17}$$

Apparently, $q^*(s)\ q(\theta)$ meets $\langle q^*(s), q(\theta)\rangle = 1$ and $\langle q^*(s), \bar{q}(\theta)\rangle = 0$. When $\mu = 0$, let μ_t be the solution of Eq (B.9), we set

$$z(t) = \langle q^*, u_t\rangle,\ \ W(t,\theta) = u_t(\theta) - 2Re\{z(t)q(\theta)\}. \tag{B.18}$$

Therefore,

$$W(t,\theta) = W(z(t),\bar{z}(t),\theta), \tag{B.19}$$

$$W(z(t),\bar{z}(t),\theta) = W_{20}(\theta)\frac{z^2}{2} + W_{11}(\theta)z\bar{z} + W_{02}(\theta)\frac{\bar{z}^2}{2} + W_{30}(\theta)\frac{z^3}{6} + \cdots, \tag{B.20}$$

here, the local coordinates of center manifold C_0 corresponding to q and q^* are expressed as z and $\bar{z}$. Note that W is real if u_t is real, thus only real solutions are considered. For solution $u_t \in C_0$, since $\mu = 0$,

$$z'(t) = i\omega_{10}\tau_k z + \overline{q^*}(0)F(0, W(z,\bar{z},0)) + 2Re\{z(t)q(\theta)\}) = i\omega_{10}\tau_k z + \overline{q^*}(0)F_0(z,\bar{z}). \tag{B.21}$$

that is

$$z'(t) = i\omega_{10}\tau_k z + g(z,\bar{z}), \tag{B.22}$$

where

$$g(z,\bar{z}) = \overline{q^*}(0)F_0(z,\bar{z}) = g_{20}(\theta)\frac{z^2}{2} + g_{11}(\theta)z\bar{z} + g_{02}(\theta)\frac{\bar{z}^2}{2} + g_{21}(\theta)\frac{z^2\bar{z}}{2} + \cdots. \tag{B.23}$$

Comparing Eqs (B.18) and (B.20), one has

$$u(t) = (u_{1t}(\theta), u_{2t}(\theta)) = W(t,\theta) + 2Re\{z(t)q(\theta)\}, \tag{B.24}$$

where $q(\theta) = (1,\Delta)^T e^{i\omega_{10}\tau_k\theta}$, furthermore

$$\begin{aligned}u_{1t}(0) &= W^{(1)}(t,0) + z + \bar{z},\\ u_{2t}(0) &= W^{(2)}(t,0) + \Delta z + \bar{\Delta}\bar{z},\\ u_{1t}(-1) &= W^{(1)}(t,-1) + ze^{-i\omega_{10}\tau_k} + \bar{z}e^{i\omega_{10}\tau_k}.\end{aligned} \tag{B.25}$$

Combining Eqs (B.3) and (B.4), we obtain

$$\begin{aligned}
g(z,\bar{z}) =&\overline{q^*}(0)F_0(z,\bar{z}) = \overline{q^*}(0)F(0,u_t) = \bar{\mathcal{D}}\tau_k(1,\overline{\Delta^*})\begin{pmatrix} F_1 \\ F_2 \end{pmatrix} = \bar{\mathcal{D}}\tau_k(F_1+\overline{\Delta^*}F_2)\\
=&\bar{\mathcal{D}}\tau_k\Big\{\Big(\frac{cy_1^*}{\mu_1^2}-\frac{cx_1^*y_1^*}{\mu_1^3}\Big)(W^{(1)}(0)+z+\bar{z})^2-(W^{(1)}(-1)+ze^{-i\omega_{10}\tau_k}+\bar{z}e^{i\omega_{10}\tau_k})^2\\
&+\Big(\frac{cx_1^*}{\mu_1^2}-\frac{cx_1^*y_1^*}{\mu_1^3}\Big)(W^{(2)}(0)+\Delta z+\bar{\Delta}\bar{z})^2\\
&+\Big(-\frac{c\alpha\xi}{\mu_1^2}-\frac{2cx_1^*y_1^*}{\mu_1^3}\Big)(W^{(1)}(0)+z+\bar{z})(W^{(2)}(0)+\Delta z+\bar{\Delta}\bar{z})\\
&+\Big(-\frac{cy_1^*}{\mu_1^3}+\frac{cx_1^*y_1^*}{\mu_1^4}\Big)(W^{(1)}(0)+z+\bar{z})^3+\Big(-\frac{cx_1^*}{\mu_1^3}+\frac{cx_1^*y_1^*}{\mu_1^4}\Big)(W^{(2)}(0)+\Delta z+\bar{\Delta}\bar{z})^3\\
&+\Big(-\frac{c(y_1^*-\alpha\xi)}{\mu_1^3}+\frac{3cx_1^*y_1^*}{\mu_1^4}\Big)(W^{(1)}(0)+z+\bar{z})^2(W^{(2)}(0)+\Delta z+\bar{\Delta}\bar{z})\\
&+\Big(-\frac{c(x_1^*-\alpha\xi)}{\mu_1^3}+\frac{3cx_1^*y_1^*}{\mu_1^4}\Big)(W^{(1)}(0)+z+\bar{z})(W^{(2)}(0)+\Delta z+\bar{\Delta}\bar{z})^2\\
&+\overline{\Delta^*}\Big(-\frac{by_1^*}{\mu_1^2}+\frac{b(x_1^*+\xi)y_1^*}{\mu_1^3}\Big)(W^{(1)}(0)+z+\bar{z})^2\\
&+\overline{\Delta^*}\Big(-\frac{b(x_1^*+\xi)}{\mu_1^2}+\frac{b(x_1^*+\xi)y_1^*}{\mu_1^3}-\frac{p^2q^3Qy_1^*}{\nu_1^3}+\frac{pq^2Q}{\nu_1^2}\Big)(W^{(2)}(0)+\Delta z+\bar{\Delta}\bar{z})^2\\
&+\overline{\Delta^*}\Big(\frac{b(\alpha\xi-\xi)}{\mu_1^2}+\frac{2b(x_1^*+\xi)y_1^*}{\mu_1^3}\Big)(W^{(1)}(0)+z+\bar{z})(W^{(2)}(0)+\Delta z+\bar{\Delta}\bar{z})\\
&+\overline{\Delta^*}\Big(\frac{by_1^*}{\mu_1^3}-\frac{b(x_1^*+\xi)y_1^*}{\mu_1^4}\Big)(W^{(1)}(0)+z+\bar{z})^3\\
&+\overline{\Delta^*}\Big(\frac{b(x_1^*+\xi)}{\mu_1^3}-\frac{b(x_1^*+\xi)y_1^*}{\mu_1^4}-\frac{p^2q^3Q}{\nu_1^3}+\frac{p^3q^4Qy_1^*}{\nu_1^4}\Big)(W^{(2)}(0)+\Delta z+\bar{\Delta}\bar{z})^3\\
&+\overline{\Delta^*}\Big(\frac{b(y_1^*-\alpha\xi+\xi)}{\mu_1^3}-\frac{3b(x_1^*+\xi)y_1^*}{\mu_1^4}\Big)(W^{(1)}(0)+z+\bar{z})^2(W^{(2)}(0)+\Delta z+\bar{\Delta}\bar{z})\\
&+\overline{\Delta^*}\Big(\frac{b(x_1^*+2\xi-\alpha\xi)}{\mu_1^3}-\frac{3b(x_1^*+\xi)y_1^*}{\mu_1^4}\Big)(W^{(1)}(0)+z+\bar{z})(W^{(2)}(0)+\Delta z+\bar{\Delta}\bar{z})^2+\cdots\Big\}\\
=&\bar{\mathcal{D}}\tau_k\Big\{2\Big(\frac{cy_1^*}{\mu_1^2}-\frac{cx_1^*y_1^*}{\mu_1^3}\Big)-2e^{-2i\omega_{10}\tau_k}+2\Delta^2\Big(\frac{cx_1^*}{\mu_1^2}-\frac{cx_1^*y_1^*}{\mu_1^3}\Big)+2\Delta\Big(-\frac{c\alpha\xi}{\mu_1^2}-\frac{2cx_1^*y_1^*}{\mu_1^3}\Big)\\
&+2\overline{\Delta^*}\Big(-\frac{by_1^*}{\mu_1^2}+\frac{b(x_1^*+\xi)y_1^*}{\mu_1^3}\Big)+2\Delta\overline{\Delta^*}\Big(\frac{b(\alpha\xi-\xi)}{\mu_1^2}+\frac{2b(x_1^*+\xi)y_1^*}{\mu_1^3}\Big)\\
&+2\Delta^2\overline{\Delta^*}\Big(-\frac{b(x_1^*+\xi)}{\mu_1^2}+\frac{b(x_1^*+\xi)y_1^*}{\mu_1^3}-\frac{p^2q^3Qy_1^*}{\nu_1^3}+\frac{pq^2Q}{\nu_1^2}\Big)\Big\}\frac{z^2}{2}+\bar{\mathcal{D}}\tau_k\Big\{2\Big(\frac{cy_1^*}{\mu_1^2}-\frac{cx_1^*y_1^*}{\nu_1^3}\Big)\\
&+2\Delta\bar{\Delta}\Big(\frac{cx_1^*}{\mu_1^2}-\frac{cx_1^*y_1^*}{\mu_1^3}\Big)+2Re(\Delta)\Big(-\frac{c\alpha\xi}{\mu_1^2}-\frac{2cx_1^*y_1^*}{\mu_1^3}\Big)-2+2\overline{\Delta^*}\Big(-\frac{by_1^*}{\mu_1^2}+\frac{b(x_1^*+\xi)y_1^*}{\mu_1^3}\Big)\\
&+2\Delta\bar{\Delta}\overline{\Delta^*}\Big(-\frac{b(x_1^*+\xi)}{\mu_1^2}+\frac{b(x_1^*+\xi)y_1^*}{\mu_1^3}-\frac{p^2q^3Qy_1^*}{\nu_1^3}+\frac{pq^2Q}{\nu_1^2}\Big)
\end{aligned}$$

$$
\begin{aligned}
&+ 2Re(\Delta)\overline{\Delta^*}\Big(\frac{b(\alpha\xi-\xi)}{\mu_1^2} + \frac{2b(x_1^*+\xi)y_1^*}{\mu_1^3}\Big)\Big\}z\bar{z} + \bar{\mathcal{D}}\tau_k\Big\{2\Big(\frac{cy_1^*}{\mu_1^2} - \frac{cx_1^*y_1^*}{\mu_1^3}\Big) - 2e^{2i\omega_{10}\tau_k}\\
&+ 2\bar{\Delta}^2\Big(\frac{cx_1^*}{\mu_1^2} - \frac{cx_1^*y_1^*}{\mu_1^3}\Big) + 2\bar{\Delta}\Big(-\frac{c\alpha\xi}{\mu_1^2} - \frac{2cx_1^*y_1^*}{\mu_1^3}\Big) + 2\overline{\Delta^*}\Big(-\frac{by_1^*}{\mu_1^2} + \frac{b(x_1^*+\xi)y_1^*}{\mu_1^3}\Big)\\
&+ 2\bar{\Delta}^2\overline{\Delta^*}\Big(-\frac{b(x_1^*+\xi)}{\mu_1^2} + \frac{b(x_1^*+\xi)y_1^*}{\mu_1^3} - \frac{p^2q^3Qy_1^*}{\nu_1^3} + \frac{pq^2Q}{\nu_1^2}\Big)\\
&+ 2\bar{\Delta}\overline{\Delta^*}\Big(\frac{b(\alpha\xi-\xi)}{\mu_1^2} + \frac{2b(x_1^*+\xi)y_1^*}{\mu_1^3}\Big)\Big\}\frac{\bar{z}^2}{2} + \bar{\mathcal{D}}\tau_k\Big\{2\Big(\frac{cy_1^*}{\mu_1^2} - \frac{cx_1^*y_1^*}{\mu_1^3}\Big)(2W_{11}^{(1)}(0) + W_{20}^{(1)}(0))\\
&- (4W_{11}^{(1)}(-1)e^{-i\omega_{10}\tau_k} + 2W_{20}^{(1)}(-1)e^{i\omega_{10}\tau_k}) + 2\Big(\frac{cx_1^*}{\mu_1^2} - \frac{cx_1^*y_1^*}{\mu_1^3}\Big)(2W_{11}^{(2)}(0)\Delta + W_{20}^{(2)}(0)\bar{\Delta})\\
&+ 2\Big(-\frac{c\alpha\xi}{\mu_1^2} - \frac{2cx_1^*y_1^*}{\mu_1^3}\Big)\Big(W_{11}^{(1)}(0)\Delta + \frac{1}{2}W_{20}^{(1)}(0)\bar{\Delta} + W_{11}^{(2)}(0) + \frac{1}{2}W_{20}^{(2)}(0)\Big)\\
&+ 6\Big(-\frac{cy_1^*}{\mu_1^3} + \frac{cx_1^*y_1^*}{\mu_1^4}\Big) + 2\overline{\Delta^*}\Big(-\frac{by_1^*}{\mu_1^2} + \frac{b(x_1^*+\xi)y_1^*}{\mu_1^3}\Big)(2W_{11}^{(1)}(0) + W_{20}^{(1)}(0))\\
&+ 2\Big(-\frac{c(x_1^*-\alpha\xi)}{\mu_1^3} + \frac{3cx_1^*y_1^*}{\mu_1^4}\Big)(2\Delta\bar{\Delta} + \Delta^2) + 6\Big(-\frac{cx_1^*}{\mu_1^3} + \frac{cx_1^*y_1^*}{\mu_1^4}\Big)(\Delta^2\bar{\Delta})\\
&+ 2\overline{\Delta^*}\Big(-\frac{b(x_1^*+\xi)}{\mu_1^2} + \frac{b(x_1^*+\xi)y_1^*}{\mu_1^3} - \frac{p^2q^3Qy_1^*}{\nu_1^3} + \frac{pq^2Q}{\nu_1^2}\Big)(2W_{11}^{(2)}(0)\Delta + W_{20}^{(2)}(0)\bar{\Delta})\\
&+ 2\overline{\Delta^*}\Big(\frac{b(\alpha\xi-\xi)}{\mu_1^2} + \frac{2b(x_1^*+\xi)y_1^*}{\mu_1^3}\Big)(W_{11}^{(1)}(0)\Delta + \frac{1}{2}W_{20}^{(1)}(0)\bar{\Delta} + W_{11}^{(2)}(0) + \frac{1}{2}W_{20}^{(2)}(0))\\
&+ 6\overline{\Delta^*}\Big(\frac{by_1^*}{\mu_1^3} - \frac{b(x_1^*+\xi)y_1^*}{\mu_1^4}\Big) + 6\Delta^2\bar{\Delta}\overline{\Delta^*}\Big(\frac{b(x_1^*+\xi)}{\mu_1^3} - \frac{b(x_1^*+\xi)y_1^*}{\mu_1^4} - \frac{p^2q^3Q}{\nu_1^3} + \frac{p^3q^4Qy_1^*}{\nu_1^4}\Big)\\
&+ 2\overline{\Delta^*}\Big(\frac{b(y_1^*-\alpha\xi+\xi)}{\mu_1^3} - \frac{3b(x_1^*+\xi)y_1^*}{\mu_1^4}\Big)(2\Delta + \bar{\Delta}) + 2\Big(-\frac{c(y_1^*-\alpha\xi)}{\mu_1^3} + \frac{3cx_1^*y_1^*}{\mu_1^4}\Big)(\bar{\Delta} + 2\Delta)\\
&+ 2\overline{\Delta^*}\Big(\frac{b(x_1^*-\alpha\xi+2\xi)}{\mu_1^3} - \frac{3b(x_1^*+\xi)y_1^*}{\mu_1^4}\Big)(2\Delta\bar{\Delta} + \Delta^2)\Big\}\frac{z^2\bar{z}}{2} + \cdots.
\end{aligned}
\tag{B.26}
$$

Comparing with the corresponding coefficients of the Eq (B.23), it yields to

$$
\begin{aligned}
g_{20} =& \bar{\mathcal{D}}\tau_k\Big\{2\Big(\frac{cy_1^*}{\mu_1^2} - \frac{cx_1^*y_1^*}{\mu_1^3}\Big) - 2e^{-2i\omega_{10}\tau_k} + 2\Delta^2\Big(\frac{cx_1^*}{\mu_1^2} - \frac{cx_1^*y_1^*}{\mu_1^3}\Big) + 2\Delta\Big(-\frac{c\alpha\xi}{\mu_1^2} - \frac{2cx_1^*y_1^*}{\mu_1^3}\Big)\\
&+ 2\overline{\Delta^*}\Big(-\frac{by_1^*}{\mu_1^2} + \frac{b(x_1^*+\xi)y_1^*}{\mu_1^3}\Big) + 2\Delta\overline{\Delta^*}\Big(\frac{b(\alpha\xi-\xi)}{\mu_1^2} + \frac{2b(x_1^*+\xi)y_1^*}{\mu_1^3}\Big)\\
&+ 2\Delta^2\overline{\Delta^*}\Big(-\frac{b(x_1^*+\xi)}{\mu_1^2} + \frac{b(x_1^*+\xi)y_1^*}{\mu_1^3} - \frac{p^2q^3Qy_1^*}{\nu_1^3} + \frac{pq^2Q}{\nu_1^2}\Big)\Big\},
\end{aligned}
$$

$$
\begin{aligned}
g_{11} =& \bar{\mathcal{D}}\tau_k\Big\{2\Big(\frac{cy_1^*}{\mu_1^2} - \frac{cx_1^*y_1^*}{\mu_1^3}\Big) - 2 + 2\Delta\bar{\Delta}\Big(\frac{cx_1^*}{\mu_1^2} - \frac{cx_1^*y_1^*}{\mu_1^3}\Big) + 2Re(\Delta)\Big(-\frac{c\alpha\xi}{\mu_1^2} - \frac{2cx_1^*y_1^*}{\mu_1^3}\Big)\\
&+ 2\overline{\Delta^*}\Big(-\frac{by_1^*}{\mu_1^2} + \frac{b(x_1^*+\xi)y_1^*}{\mu_1^3}\Big) + 2Re(\Delta)\overline{\Delta^*}\Big(\frac{b(\alpha\xi-\xi)}{\mu_1^2} + \frac{2b(x_1^*+\xi)y_1^*}{\mu_1^3}\Big)
\end{aligned}
$$

$$
\begin{aligned}
&+2\Delta\bar{\Delta}\overline{\Delta^*}\Big(-\frac{b(x_1^*+\xi)}{\mu_1^2}+\frac{b(x_1^*+\xi)y_1^*}{\mu_1^3}-\frac{p^2q^3Qy_1^*}{\nu_1^3}+\frac{pq^2Q}{\nu_1^2}\Big)\Big\},\\
g_{02}=&\bar{\mathcal{D}}\tau_k\Big\{2\Big(\frac{cy_1^*}{\mu_1^2}-\frac{cx_1^*y_1^*}{\mu_1^3}\Big)-2e^{2i\omega_{10}\tau_k}+2\bar{\Delta}^2\Big(\frac{cx_1^*}{\mu_1^2}-\frac{cx_1^*y_1^*}{\mu_1^3}\Big)+2\bar{\Delta}\Big(-\frac{c\alpha\xi}{\mu_1^2}-\frac{2cx_1^*y_1^*}{\mu_1^3}\Big)\\
&+2\overline{\Delta^*}\Big(-\frac{by_1^*}{\mu_1^2}+\frac{b(x_1^*+\xi)y_1^*}{\mu_1^3}\Big)+2\bar{\Delta}\overline{\Delta^*}\Big(\frac{b(\alpha\xi-\xi)}{\mu_1^2}+\frac{2b(x_1^*+\xi)y_1^*}{\mu_1^3}\Big)\\
&+2\bar{\Delta}^2\overline{\Delta^*}\Big(-\frac{b(x_1^*+\xi)}{\mu_1^2}+\frac{b(x_1^*+\xi)y_1^*}{\mu_1^3}-\frac{p^2q^3Qy_1^*}{\nu_1^3}+\frac{pq^2Q}{\nu_1^2}\Big)\Big\},\\
g_{21}=&\bar{\mathcal{D}}\tau_k\Big\{2\Big(\frac{cy_1^*}{\mu_1^2}-\frac{cx_1^*y_1^*}{\mu_1^3}\Big)(2W_{11}^{(1)}(0)+W_{20}^{(1)}(0))-(4W_{11}^{(1)}(-1)e^{-i\omega_{10}\tau_k}+2W_{20}^{(1)}(-1)e^{i\omega_{10}\tau_k})\\
&+2\Big(\frac{cx_1^*}{\mu_1^2}-\frac{cx_1^*y_1^*}{\mu_1^3}\Big)(2W_{11}^{(2)}(0)\Delta+W_{20}^{(2)}(0)\bar{\Delta})+2\Big(-\frac{c(x_1^*-\alpha\xi)}{\mu_1^3}+\frac{3cx_1^*y_1^*}{\mu_1^4}\Big)(2\Delta\bar{\Delta}+\Delta^2)\\
&+2\Big(-\frac{c\alpha\xi}{\mu_1^2}-\frac{2cx_1^*y_1^*}{\mu_1^3}\Big)(W_{11}^{(1)}(0)\Delta+\frac{1}{2}W_{20}^{(1)}(0)\bar{\Delta}+W_{11}^{(2)}(0)+\frac{1}{2}W_{20}^{(2)}(0))\\
&+6\Big(-\frac{cy_1^*}{\mu_1^3}+\frac{cx_1^*y_1^*}{\mu_1^4}\Big)+6\Big(-\frac{cx_1^*}{\mu_1^3}+\frac{cx_1^*y_1^*}{\mu_1^4}\Big)(\Delta^2\bar{\Delta})+2\Big(-\frac{c(y_1^*-\alpha\xi)}{\mu_1^3}+\frac{3cx_1^*y_1^*}{\mu_1^4}\Big)(\overline{\Delta}+2\Delta)\\
&+2\overline{\Delta^*}\Big(-\frac{by_1^*}{\mu_1^2}+\frac{b(x_1^*+\xi)y_1^*}{\mu_1^3}\Big)(2W_{11}^{(1)}(0)+W_{20}^{(1)}(0))\\
&+2\overline{\Delta^*}\Big(-\frac{b(x_1^*+\xi)}{\mu_1^2}+\frac{b(x_1^*+\xi)y_1^*}{\mu_1^3}-\frac{p^2q^3Qy_1^*}{\nu_1^3}+\frac{pq^2Q}{\nu_1^2}\Big)(2W_{11}^{(2)}(0)\Delta+W_{20}^{(2)}(0)\bar{\Delta})\\
&+2\overline{\Delta^*}\Big(\frac{b(\alpha\xi-\xi)}{\mu_1^2}+\frac{2b(x_1^*+\xi)y_1^*}{\mu_1^3}\Big)(W_{11}^{(1)}(0)\Delta+\frac{1}{2}W_{20}^{(1)}(0)\bar{\Delta}+W_{11}^{(2)}(0)+\frac{1}{2}W_{20}^{(2)}(0))\\
&+6\overline{\Delta^*}\Big(\frac{by_1^*}{\mu_1^3}-\frac{b(x_1^*+\xi)y_1^*}{\mu_1^4}\Big)+6\Delta^2\bar{\Delta}\overline{\Delta^*}\Big(\frac{b(x_1^*+\xi)}{\mu_1^3}-\frac{b(x_1^*+\xi)y_1^*}{\mu_1^4}-\frac{p^2q^3Q}{\nu_1^3}+\frac{p^3q^4Qy_1^*}{\nu_1^4}\Big)\\
&+2\overline{\Delta^*}\Big(\frac{b(y_1^*-\alpha\xi+\xi)}{\mu_1^3}-\frac{3b(x_1^*+\xi)y_1^*}{\mu_1^4}\Big)(2\Delta+\bar{\Delta})\\
&+2\overline{\Delta^*}\Big(\frac{b(x_1^*-\alpha\xi+2\xi)}{\mu_1^3}-\frac{3b(x_1^*+\xi)y_1^*}{\mu_1^4}\Big)(2\Delta\bar{\Delta}+\Delta^2)\Big\}.
\end{aligned}
\tag{B.27}
$$

In order to deduce g_{21}, now we have to calculate $W_{20}(\theta)$ and $W_{10}(\theta)$. It follows from Eqs (B.9) and (B.18) that

$$
\begin{aligned}
W' = u_t' - z'q - \bar{z}'\bar{q} &= \begin{cases} \mathcal{A}W - 2Re\{\overline{q^*}(0)F_0 q(\theta), & -1 \le \theta < 0, \\ \mathcal{A}W - 2Re\{\overline{q^*}(0)F_0 q(\theta) + F_0, & \theta = 0, \end{cases}\\
&:= \mathcal{A}W + H(z,\bar{z},\theta),
\end{aligned}
\tag{B.28}
$$

where

$$
H(z,\bar{z},\theta) = H_{20}(\theta)\frac{z^2}{2} + H_{11}(\theta)z\bar{z} + H_{02}(\theta)\frac{\bar{z}^2}{2} + \cdots. \tag{B.29}
$$

Consider on the center manifold C_0 close enough to the origin, we have

$$
\dot{W} = W_z\dot{z} + W_{\bar{z}}\dot{\bar{z}}. \tag{B.30}
$$

Substituting Eq (B.30) into (B.28) and comparing the coefficients on z^2 and $z\bar{z}$, it easy to see

$$\begin{aligned}&(\mathcal{A}-2i\omega_{10}\tau_k I)W_{20}(\theta)=-H_{20}(\theta),\\&\mathcal{A}W_{11}(\theta)=-H_{11}(\theta).\end{aligned}\tag{B.31}$$

For $\theta\in[-1,0)$, from Eq (B.28) we can get

$$H(z,\bar{z},\theta)=-\overline{q^*}(0)F_0q(\theta)-q^*(0)\bar{F}_0\bar{q}(\theta)=-gq(\theta)-\bar{g}\bar{q}(\theta).\tag{B.32}$$

Comparing the coefficients of Eq (B.29) gives that

$$\begin{aligned}&H_{20}(\theta)=-g_{20}q(\theta)-\bar{g}_{02}\bar{q}(\theta),\\&H_{11}(\theta)=-g_{11}q(\theta)-\bar{g}_{11}\bar{q}(\theta).\end{aligned}\tag{B.33}$$

We have from Eqs (B.31) and (B.33) that

$$\dot{W}_{20}(\theta)=2i\omega_{10}\tau_kW_{20}(\theta)+g_{20}q(\theta)+\bar{g}_{02}\bar{q}(\theta).\tag{B.34}$$

Noticing that $q(\theta)=q(0)e^{i\omega_{10}\tau_k\theta}$, then

$$W_{20}(\theta)=\frac{ig_{20}}{\omega_{10}\tau_k}q(0)e^{i\omega_{10}\tau_k\theta}+\frac{i\bar{g}_{02}}{3\omega_{10}\tau_k}\bar{q}(0)e^{-i\omega_{10}\tau_k\theta}+M_1e^{2i\omega_{10}\tau_k\theta},\tag{B.35}$$

where $M_1=(M_1^{(1)},M_1^{(2)})\in\mathbb{R}^2$ is a constant vector. By the same method as that in the above part we can calculate

$$W_{11}(\theta)=-\frac{ig_{11}}{\omega_{10}\tau_k}q(0)e^{i\omega_{10}\tau_k\theta}+\frac{i\bar{g}_{11}}{\omega_{10}\tau_k}\bar{q}(0)e^{-i\omega_{10}\tau_k\theta}+M_2,\tag{B.36}$$

where $M_2=(M_2^{(1)},M_2^{(2)})\in\mathbb{R}^2$ is also a constant vector.

Calculating constant vectors M_1 and M_2 is our main work in the following discussion. It follows from Eqs (B.28) and (B.29) that

$$\begin{aligned}&H_{20}(0)=-g_{20}q(0)-\bar{g}_{02}\bar{q}(0)+2\tau_kN_1,\\&H_{11}(0)=-g_{11}q(0)-\bar{g}_{11}\bar{q}(0)+2\tau_kN_2,\end{aligned}\tag{B.37}$$

where

$$N_1=\begin{pmatrix}a_{11}\\a_{22}\end{pmatrix},\quad N_2=\begin{pmatrix}b_{11}\\b_{22}\end{pmatrix},\tag{B.38}$$

and

$$\begin{aligned}a_{11}=&\Big(\frac{cy_1^*}{\mu_1^2}-\frac{cx_1^*y_1^*}{\mu_1^3}\Big)-e^{-2i\omega_{10}\tau_k}+\Delta^2\Big(\frac{cx_1^*}{\mu_1^2}-\frac{cx_1^*y_1^*}{\mu_1^3}\Big)+\Delta\Big(-\frac{c\alpha\xi}{\mu_1^2}-\frac{2cx_1^*y_1^*}{\mu_1^3}\Big),\\a_{22}=&\Big(-\frac{by_1^*}{\mu_1^2}+\frac{b(x_1^*+\xi)y_1^*}{\mu_1^3}\Big)+\Delta^2\Big(-\frac{b(x_1^*+\xi)}{\mu_1^2}+\frac{b(x_1^*+\xi)y_1^*}{\mu_1^3}-\frac{p^2q^3Qy_1^*}{\nu_1^3}+\frac{pq^2Q}{\nu_1^2}\Big)\\&+\Delta\Big(\frac{b(\alpha\xi-\xi)}{\mu_1^2}+\frac{2b(x_1^*+\xi)y_1^*}{\mu_1^3}\Big),\\b_{11}=&\Big(\frac{cy_1^*}{\mu_1^2}-\frac{cx_1^*y_1^*}{\mu_1^3}\Big)-1+\Delta\bar{\Delta}\Big(\frac{cx_1^*}{\mu_1^2}-\frac{cx_1^*y_1^*}{\mu_1^3}\Big)+Re(\Delta)\Big(-\frac{c\alpha\xi}{\mu_1^2}-\frac{2cx_1^*y_1^*}{\mu_1^3}\Big),\\b_{22}=&\Big(-\frac{by_1^*}{\mu_1^2}+\frac{b(x_1^*+\xi)y_1^*}{\mu_1^3}\Big)+\Delta\bar{\Delta}\Big(-\frac{b(x_1^*+\xi)}{\mu_1^2}+\frac{b(x_1^*+\xi)y_1^*}{\mu_1^3}-\frac{p^2q^3Qy_1^*}{\nu_1^3}+\frac{pq^2Q}{\nu_1^2}\Big)\\&+Re(\Delta)\Big(\frac{b(\alpha\xi-\xi)}{\mu_1^2}+\frac{2b(x_1^*+\xi)y_1^*}{\mu_1^3}\Big).\end{aligned}$$

According to the definition of $\mathcal{A}$ and Eq (B.31) we have

$$\int_{-1}^{0} d\eta(\theta)W_{20}(\theta) = 2i\omega_{10}\tau_k W_{20}(0) - H_{20}(0) \tag{B.39}$$

and

$$\int_{-1}^{0} d\eta(\theta)W_{11}(\theta) = -H_{11}(0), \tag{B.40}$$

where $\eta(\theta) = \eta(0, \theta)$. Substituting Eqs (B.35), (B.36) and (B.37) into (B.31), we notice that

$$\left(i\omega_{10}\tau_k I - \int_{-1}^{0} e^{i\omega_{10}\tau_k\theta} d\eta(\theta)\right)q(0) = 0, \tag{B.41}$$

$$\left(-i\omega_{10}\tau_k I - \int_{-1}^{0} e^{-i\omega_{10}\tau_k\theta} d\eta(\theta)\right)\bar{q}(0) = 0, \tag{B.42}$$

it is easy to see

$$\left(2i\omega_{10}\tau_k I - \int_{-1}^{0} e^{2i\omega_{10}\tau_k\theta} d\eta(\theta)\right)M_1 = 2\tau_k N_1, \tag{B.43}$$

$$\int_{-1}^{0} d\eta(\theta)M_2 = -2\tau_k N_2. \tag{B.44}$$

Hence, we further get

$$M_1 = 2\begin{pmatrix} 2i\omega_{10} - \dfrac{cx_1^* y_1^*}{\mu_1^2} + x_1^* e^{-2i\omega_{10}\tau_k} & \dfrac{cx_1^*(x_1^* + \alpha\xi)}{\mu_1^2} \\ -\dfrac{by_1^*(y_1^* + \alpha\xi - \xi)}{\mu_1^2} & 2i\omega_{10} + \dfrac{b(x_1^* + \xi)y_1^*}{\mu_1^2} - \dfrac{pq^2E^* y_1*}{\nu_1} \end{pmatrix}^{-1} N_1 \tag{B.45}$$

and

$$M_2 = 2\begin{pmatrix} \dfrac{cx_1^* y_1^*}{\mu_1^2} + x_1^* & -\dfrac{cx_1^*(x_1^* + \alpha\xi)}{\mu_1^2} \\ \dfrac{by_1^*(y_1^* + \alpha\xi - \xi)}{\mu_1^2} & -\dfrac{b(x_1^* + \xi)y_1^*}{\mu_1^2} + \dfrac{pq^2E^* y_1*}{\nu_1} \end{pmatrix}^{-1} N_2. \tag{B.46}$$

From Eqs (B.35) and (B.36), we can determine the values of $W_{20}(\theta)$ and $W_{11}(\theta)$. g_{21} be represented by the parameters of Eq (B.1). Therefore, we further calculate the values of $c_1(0), \mu_2, \beta_2$ and T_2, as follows

$$\begin{aligned} c_1(0) &= \frac{i}{2\omega_{10}\tau_k}\left(g_{20}g_{11} - 2|g_{11}|^2 - \frac{|g_{02}|^2}{3}\right) + \frac{g_{21}}{2}, \\ \mu_2 &= -\frac{Re\{c_1(0)\}}{Re\{\lambda'(\tau_k)\}}, \quad \beta_2 = 2Re\{c_1(0)\}, \\ T_2 &= \frac{Im\{c_1(0)\} + \mu_2 Im\{\lambda'(\tau_k)\}}{\omega_{10}\tau_k}. \end{aligned} \tag{B.47}$$

Appendix C

Before finding the maximum value of $\mathcal{J}(E)$, the concrete Hamiltonian function is given

$$\begin{aligned} H =& E(p_1q_1P - w)e^{-\delta t} \\ &+\lambda_1\Big(rN(1-\frac{N}{K}) - \frac{e_1(\frac{N}{P})}{1+e_1h_1(\frac{N}{P})+e_2h_2(\frac{A}{P})}P\Big) \\ &+\lambda_2\Big(\frac{n_1e_1(\frac{N}{P})+n_2e_2(\frac{A}{P})}{1+e_1h_1(\frac{N}{P})+e_2h_2(\frac{A}{P})}P - m'P - q_1EP\Big). \end{aligned} \tag{C.4}$$

where $\lambda_i = \lambda_i(t), i = 1, 2$, are adjoint variables. The condition that the Hamiltonian function H satisfy is presented by

$$\frac{\partial H}{\partial E} = (p_1q_1P - w)e^{-\delta t} - \lambda_2 q_1 P = 0, \tag{C.5}$$

The adjoint variables λ_1 and λ_2 satisfy the following adjoint equations according to Pontryagin's Maximum Principle.

$$\begin{aligned} \frac{d\lambda_1}{dt} &= -\frac{\partial H}{\partial N} = \lambda_1\Big(\frac{rN}{K} - \frac{e_1^2h_1\frac{N}{P}}{(1+e_1h_1\frac{N}{P}+e_2h_2\frac{A}{P})^2}\Big) - \lambda_2\Big(\frac{n_1e_1(1+e_2h_2\frac{A}{P}) - e_1e_2h_1n_2\frac{A}{P}}{(1+e_1h_1\frac{N}{P}+e_2h_2\frac{A}{P})^2}\Big), \\ \frac{d\lambda_2}{dt} &= -\frac{\partial H}{\partial P} = -p_1q_1Ee^{-\delta t} + \lambda_1\Big(\frac{e_1\frac{N}{P}(e_1h_1\frac{N}{P}+e_2h_2\frac{A}{P})}{(1+e_1h_1\frac{N}{P}+e_2h_2\frac{A}{P})^2}\Big) + \lambda_2\Big(\frac{e_1n_1\frac{N}{P}+e_2n_2\frac{A}{P}}{(1+e_1h_1\frac{N}{P}+e_2h_2\frac{A}{P})^2}\Big). \end{aligned} \tag{C.6}$$

In order to find the solutions $\lambda_1(t)$, $\lambda_2(t)$ of Eq (C.6), we delete λ_2 in Eq (C.6) to obtain a second order differential equation with respect to λ_1

$$\frac{d^2\lambda_1}{dt^2} + I_1\frac{d\lambda_1}{dt} + I_2\lambda_1 = C_1e^{-\delta t}, \tag{C.7}$$

where

$$\begin{aligned} I_1 =& -\Big(\frac{rN}{K} - \frac{e_1^2h_1\frac{N}{P}}{(1+e_1h_1\frac{N}{P}+e_2h_2\frac{A}{P})^2}\Big) - \frac{e_1n_1\frac{N}{P}+e_2n_2\frac{A}{P}}{(1+e_1h_1\frac{N}{P}+e_2h_2\frac{A}{P})^2}, \\ I_2 =& \frac{(n_1e_1+e_1e_2n_1h_2\frac{A}{P} - e_1e_2n_2h_1\frac{A}{P})(e_1^2h_1\frac{N^2}{P^2}+e_1e_2h_2\frac{AN}{P^2})}{(1+e_1h_1\frac{N}{P}+e_2h_2\frac{A}{P})^4} \\ &+ \frac{e_1n_1\frac{N}{P}+e_2n_2\frac{A}{P}}{(1+e_1h_1\frac{N}{P}+e_2h_2\frac{A}{P})^2}\Big(\frac{rN}{K} - \frac{e_1^2h_1\frac{N}{P}}{(1+e_1h_1\frac{N}{P}+e_2h_2\frac{A}{P})^2}\Big), \\ C_1 =& \frac{(n_1e_1(1+e_2h_2\frac{A}{P}) - e_1e_2n_2h_1\frac{A}{P})Ep_1q_1}{(1+e_1h_1\frac{N}{P}+e_2h_2\frac{A}{P})^2}. \end{aligned} \tag{C.8}$$

Then, we obtain $\lambda_1(t) = O_1e^{-\delta t}$, where $O_1 = \frac{C_1}{\delta^2 - I_1\delta + I_2}$. Set up the equation in a similar way as above $\frac{d^2\lambda_2}{dt^2} + I_1\frac{d\lambda_2}{dt} + I_2\lambda_1 = C_2e^{-\delta t}$, we get $\lambda_2(t) = O_2e^{-\delta t}$, where $O_2 = \frac{C_2}{\delta^2 - I_1\delta + I_2}$, $C_2 = -Ep_1q_1\Big(\delta + \frac{rN}{K} - \frac{e_1^2h_1\frac{N}{P}}{(1+e_1h_1\frac{N}{P}+e_2h_2\frac{A}{P})^2}\Big)$. Substituting $\lambda_2(t)$ into (C.5) yields

$$E = \frac{(\delta^2 - I_1\delta + I_2)(p_1q_1P - w)}{\Big(p_1q_1\delta + p_1q_1\frac{rN}{K} - \frac{e_1^2h_1p_1q_1\frac{N}{P}}{(1+e_1h_1\frac{N}{P}+e_2h_2\frac{A}{P})^2}\Big)q_1P}. \tag{C.9}$$

Therefore, the values of $(N^{optimal}, P^{optimal})$ and $E^{optimal}$ can be obtained by Eq (C.9) and solving the biological equilibrium.

The optimal harvesting effort at any time is determined by the following optimal harvesting solution

$$E(t) = \begin{cases} E^{max} & \text{if } \frac{\partial H}{\partial E} > 0, \\ E^{optimal} & \text{if } \frac{\partial H}{\partial E} = 0, \\ E^{min} & \text{if } \frac{\partial H}{\partial E} < 0, \end{cases} \tag{C.10}$$

where E^{min} is the minimum harvesting effort.